

MESTRADO

MEDICINA E ONCOLOGIA MOLECULAR

Role of BRCA1-A and BRCA1-B complexes in DNA repair pathway choice and in replication stress

Mariana Paes Lobo Lopes Dias

M

2017





Telomere Damage and Cancer Group

Netherlands Cancer Institute (NKI)

Supervisor

Dr Jacqueline Jacobs, PhD

Group leader of the Telomere Damage and Cancer Group

Department of Molecular Oncology of the Netherlands Cancer Institute

Co-supervisor

Dr Marco Simonetta, PhD

Postdoctoral Fellow in the Telomere Damage and Cancer Group

Department of Molecular Oncology of the Netherlands Cancer Institute

Acknowledgments

To Dr Jacqueline Jacobs for allowing me to carry out this internship in her lab and for trusting me with this project, for her supervision and for the constructive work discussions.

To Dr Marco Simonetta for his direct supervision, for the guidance and support, and for all the knowledge and wise advices he has given to me throughout this internship.

To Aurora Cerutti, Inge de Krijger, Judit Serrat, Vera Boersma, and Zeliha Yalcin, Diogo Fortunato, Tijmen van Dam and Mathias Eder for their support and help, and for all the constructive work discussions.

To the Medema and Rowland labs for providing the pDonor plasmid and for the interesting weekly work discussions in the Medema-Rowland-Jacobs group meetings.

To the Bioimaging facility of the NKI-AvL for all the help and for providing tools that greatly facilitate in-house research.

Table of Contents

Figure Index	iii
Abbreviations	vi
Abstract	ix
Resumo	x
1. Introduction	1
1.1. DNA double-strand break repair pathway choice.....	1
1.2. Targeting Poly (ADP-ribose) polymerase (PARP) 1 in BRCA1 -deficient tumors	3
1.3. Mechanisms of resistance to PARPi in BRCA1-deficient tumors	4
1.4. BRCA1: a master regulator of genome integrity	5
1.5. Roles of BRCA1-A and -B complexes	7
2. Objectives	8
2.1. Main Objective	8
2.2. Specific Objectives.....	8
3. Materials and Methods	9
3.1. Cell culture and clonogenic survival assays.....	9
3.2. Cloning and CRISPR–Cas9 genome editing.....	9
3.3. shRNA-mediated silencing	10
3.4. Transfections and lentiviral infections	10
3.5. DNA extraction and PCR.....	11
3.6. Protein extraction and Western Blot	11
3.7. Immunofluorescence	12
4. Results	13
4.1. Generation of knockout clones of <i>ABRAXAS</i> and <i>BRIP1</i>	13
4.2. Sensitivity of knockout clones to Olaparib.....	14
4.3. Analysis of the DNA repair pathway choice upon Abraxas and BRIP1 depletion	15
4.4. Analysis of replication stress after treatment with hydroxyurea	22
5. Discussion	25
6. Conclusion and Future Perspectives	29
7. References	30

Figure Index

Figure 1- Repair of DSBs by NHEJ and by HDR. **a)** NHEJ operates throughout the cell cycle, being particularly important in G1. 53BP1 inhibits 5' end resection through the recruitment of RIF1 and the downstream protein MAD2L2, preventing the promotion of HDR by BRCA1 while committing to NHEJ repair. Inhibition of 5' end resection allows the KU70– KU80 complex, DNA-PKcs and the XRCC4–XLF–DNA ligase IV complex to localize at DSBs, leading to ligation of the broken ends by DNA ligase IV. **b)** HDR is restricted to the S and G2 phases of the cell cycle. It is initiated when BRCA1 is able to stimulate 5' end resection by releasing the inhibitory effect of 53BP1. CtIP then promotes 5' end resection through the interaction with the MRN complex and stimulation of its nuclease activity. End resection inhibits the binding of KU70–KU80 to DNA ends, thereby also inhibiting NHEJ. RPA rapidly coats the ssDNA generated by DNA end resection and is then replaced by the recombinase RAD51, a process dependent on BRCA2. RAD51 filament formation enables homology search, duplex invasion and DNA synthesis. Adapted from Panier and Durocher, 2013²⁰ 2

Figure 2 - Genetic concept of synthetic lethality and PARP1 inhibition in BRCA1-deficient cells. **a)** A genetic interaction in which single-gene defects are compatible with cell viability, but the combination of gene effects results in cell death. The first clinical exemplification of synthetic lethality in cancer was the targeting of BRCA-deficient tumor cells with PARPi. **b)** PARP1 is involved in the repair of SSBs. Upon damage, PARP1 is recruited to the site of SSBs, where it binds DNA and catalyses a series of PARylation events, promoting DNA repair. As part of this process, PARP1 autoPARylates, leading to its release from DNA. PARPi prevent the release of PARP1 from DNA, most likely by inhibiting autoPARylation. PARP1 autoPARylates, leading to its release from DNA. PARPi prevent release of PARP1 from DNA, most likely by inhibiting autoPARylation. PARP1 inhibition leads to the stalling of the replication fork by accumulation of SSbs, ultimately leading to the collapse of the RF, causing DSBs). **c)** Cells repair the RF preferably by HDR. Cells deficient in BRCA1 have a dysfunctional HDR and, therefore, the number of stalled RFs accumulates. Cells use alternative error-prone repair mechanisms, such as NHEJ, which are incapable of efficiently repairing the RF, resulting in chromosomal instability and subsequent cell death. This defect results in a hypersensitivity of BRCA1-deficient cells to PARPi. Adapted from Lord and Ashworth, 2013²¹ 4

Figure 3 – BRCA1 Complexes. BRCA1-A complex is composed of BRCA1, RAP80, Abraxas, MERIT40, BRCC45, and BRCC36. BRCA1-B is composed of BRCA1, TopBP1, and BRIP1. BRCA1-C comprises BRCA1, CtIP and MRE11–RAD50–NBS1 complex (MRN complex)..... 6

Figure 4 – Identification of Abraxas and BRIP1 knockout clones in HeLa cells. **a)** Schematic representation of our CRISPR-Cas9 approach. Adapted from Lackner et al. 2015⁶³. **b)** Exemplification of how a PCR followed by agarose gel electrophoresis can identify knockout clones. For comparison, PCR products from a control, a knockout (BRIP1 KO # 8-7), and heterozygous sample are shown. Blue arrow indicates the size of the fragments without tag insertion, and orange arrow indicates the size of the fragments with tag insertion. Samples that only display a band, corresponding to the upper

fragment (with insertion of tag), have the targeting gene disrupted. Samples that exhibit both fragments don't have tag insertion in all alleles and, thus, were considered to be heterozygous and discarded. c), d) Western-blot analysis representing protein expression of knockout clones of Abraxas and BRIP1, respectively. For comparison, samples from a control, knockout and heterozygous clones are shown. Histone H2B was blotted as a loading control. 14

Figure 5 – Sensitivity to Olaparib. a) Crystal violet staining of untransduced HeLa cells, HeLa cells transduced with shBRCA1 lentivirus particles, and Abraxas and BRIP1 knockout clones treated with DMSO (vehicle) or Olaparib (1µM) during 12 days. b) Quantification of cell survival from a) by measurement of extracted crystal violet absorbance at 590 nm. Graph shows cell survival ratio between Olaparib and DMSO treatment. All values were normalized by the mean of the blank. Mean is shown from three independent measurements. 15

Figure 6 – 53BP1 and RIF1 foci formation. a) Representative images of 53BP1 and b) RIF1 nuclear foci in the indicated cells, 3h after exposure to ionizing radiation (5 Gy), visualized by immunofluorescence. The cells shown were consider to express high CENPF indicating to be in the S/G2 of the cell cycle. Scale bar: 14µm. c) Quantification of 53BP1 and d) RIF1 foci in more than 100 cells exposed to 5 Gy, per condition. Each dot represents one cell (n=1; mean ± s.d.). Statistical analysis was performed in GraphPad Prism 7 using a two-way ANOVA test. Results from statistical analysis of “High CENPF” group are displayed in the graphic. n.s., not significant; *, P < 0.05; **, P < 0.01 ; ****, P < 0.0001. 17

Figure 7- Clonogenic assay in the presence of 3µM Olaparib at the time of experiments from Fig.6. a) Crystal violet staining of untransduced HeLa cells, HeLa cells transduced with shBRCA1 lentivirus particles, and Abraxas and BRIP1 knockout clones clones treated with DMSO (vehicle) or Olaparib (3µM) during 12 days. b) Quantification of cell survival from a) by measurement of absorbance extracted crystal violet at 590 nm. Graph shows cell survival ratio between Olaparib and DMSO treatment. All values were normalized by the mean of the blank. Mean is shown from three independent measurements. 18

Figure 8- Knockdown of 53BP1 in knockout clones. a) Crystal violet staining of untransduced HeLa cells, HeLa cells transduced with shBRCA1 lentivirus particles, and Abraxas and BRIP1 knockout clones treated with DMSO (vehicle) or Olaparib (3µM) during 12 days, upon 53BP1 knockdown. b) Quantification of cell survival from a) by measurement of extracted crystal violet absorbance at 590 nm. Graph shows cell survival ratio between Olaparib and DMSO treatment. All values were normalized by the mean of the blank. Mean is shown from three independent measurements. c) Protein expression analysis by western blot of the cells analyzed in a). Histone H3 was blotted as a loading control. LE, low exposure; HE, high exposure. 20

Figure 9 - Knockdown of MAD2L2 in knockout clones. a) Crystal violet staining of untransduced HeLa cells, HeLa cells transduced with shBRCA1 lentivirus particles, and Abraxas and BRIP1 knockout clones treated with DMSO (vehicle) or Olaparib (3µM) during 12 days, upon 53BP1 knockdown. b) Quantification of cell survival from a) by measurement of extracted crystal violet absorbance at 590

nm. Graph shows cell survival ratio between Olaparib and DMSO treatment. All values were normalized by the mean of the blank. Mean is shown from three independent measurements. c) Protein expression analysis by western blot of the cells analyzed in a). Histone H3 was blotted as a loading control. 21

Figure 10 - Analysis of replication stress after treatment with HU. a) Quantification of MFI of γ -H2AX. Cells untreated (NT) and cells treated with 2 mM HU were fixed after 3 hours. b) Analysis of ssDNA by quantification of the MFI of BrdU. Cells were cultured with BrdU-containing medium (10 μ g/ml) for 30h, and then released in new growth medium with, or without (NT), 2mM HU and fixed after 3h. Only cells with high CENP expression were used for calculations. More than 100 cells per condition were used for calculations. The ratio between cells treated (HU) and untreated (NT) is displayed in the graphics (mean \pm s.d.). Statistical analysis was performed in GraphPad Prism 7 using a two-way ANOVA test. Results from statistical analysis of the "High CENPF" group are displayed in the graphic. n.s., not significant; *, P < 0.05; ***, P < 0.001 ; ****, P < 0.0001. 23

Figure 11 – Clonogenic assay in the presence of 3 μ M Olaparib at the time of experiments from Fig.10. a) Crystal violet staining of untransduced HeLa cells, HeLa cells transduced with shBRCA1 lentivirus particles, and Abraxas and BRIP1 knockout clones treated with DMSO (vehicle) or Olaparib (3 μ M) during 12 days, at the time of experiment showed in Fig.10a and c) at the time of experiment showed in Fig.10b. b), d) Quantification of cell survival from a) and c), respectively, by measurement of absorbance of crystal violet at 590 nm. Graph shows cell survival ratio between Olaparib and DMSO treatment. All values were normalized by the mean of the blank. Mean is shown from three independent measurements. 24

Abbreviations

B

BRCT	BRCA1 C-terminal
BrdU	Bromodeoxyuridine

C

CDK	Cyclin-dependent kinase
CRISPR	Clustered Regularly Interspaced Short Palindromic Repeats

D

DDR	DNA damage response
DMSO	Dimethyl sulfoxide
DNA	Deoxyribonucleic acid
DNA-PKcs	DNA-dependent protein kinase, catalytic subunit
DSB	Double-strand break
DUB	Deubiquitinating enzyme

F

FA	Fanconi Anemia
----	----------------

G

Gy	Grey
----	------

H

HDR	Homologous recombination directed repair
HU	Hydroxyurea

I

ICL	Interstrand crosslink
IF	Immunofluorescence

IR	Ionizing radiation
IRIF	Ionizing radiation induced foci
LB	
LB	Luria-Bertani
K	
KO	Knockout
M	
MFI	Mean fluorescence intensity
N	
NHEJ	Non-homologous end joining
NT	Non-treated
P	
PARP	Poly (ADP-ribose) polymerase
PARPi	PARP inhibitors
PCR	Polymerase chain reaction
R	
RF	Replication fork
RING	Really interesting new gene
RNA	Ribonucleic acid
S	
sgRNA	Single-guide RNA
SSB	Single-strand break
ssDNA	single-stranded DNA

U

UIM Ubiquitin interacting motif

W

Wt Wild-type

Abstract

Germline mutations in *BRCA1* and *BRCA2* account for the vast majority of familial breast and ovarian cancer cases. Over the past 20 years, there has been considerable progress in our understanding of the biological functions of BRCA proteins, which has led to the development of new therapeutic approaches that target tumors with loss-of-function mutations in *BRCA* genes. An approach that has been used to treat these tumors is to exploit the genetic concept of synthetic lethality. Inhibition of PARP1 has been shown to be synthetically lethal with deficiency of BRCA1/2. This observation provided the impetus for PARP1 inhibitors to be tested clinically which has recently resulted in the approval of the first inhibitor, Olaparib, for the treatment of patients with germline mutations in *BRCA* genes. Although this approach has shown promise, multiple potential resistance mechanisms have been identified. In order to overcome this problem, a better understanding of BRCA1 and BRCA2's molecular functions and their binding partners is needed. BRCA proteins play a role in DNA repair pathway choice and in replication stress response, functions which are involved in sensitivity to PARP1 inhibitors. The BRCA1 protein C-terminus BRCT domains interact with multiple proteins and are required for BRCA1's tumor suppressor function. Through this domain, BRCA1 forms three mutually exclusive complexes with Abraxas, BRIP1, and CtIP, originating the BRCA1-A, -B and -C complexes, respectively. With this study, we decided to investigate the roles of BRCA1-A and -B complexes in these two mechanisms, as their role. Together, our results show that depletion of either Abraxas or BRIP1, and consequently, disruption of the respective complexes, is synthetically lethal with PARP1 inhibition. We suggest this phenotype to be a result of the role played by BRCA1-A and BRCA1-B in HDR, more specifically, in the DNA repair pathway choice. Moreover, BRIP1 expression, or the assembly of BRCA1-B, appears to influence the expression of Abraxas. Here, we also propose a role in replication stress response played by BRCA1-A and -B complexes. However, further investigation is needed to validate our findings. In a general manner, our results contribute to a full understanding of BRCA1 and its binding partners' molecular functions. This knowledge is crucial to understand the mechanisms of resistance to the current drugs used in BRCA-deficient cells, and to improve the current therapeutic approaches.

Resumo

Mutações hereditárias nos genes *BRCA1* e *BRCA2* representam a grande maioria dos casos familiares de cancro de mama e de ovário. Ao longo dos últimos 20 anos, houve um progresso considerável na compreensão das funções biológicas das proteínas BRCA, o que levou ao desenvolvimento de novas abordagens terapêuticas que visam tumores com mutações que levam à perda de função dos genes *BRCA*. Uma abordagem que tem sido usada para o tratamento deste tumores baseia-se no conceito genético de letalidade sintética. A inibição de PARP1 mostrou-se sinteticamente letal com a deficiência de BRCA1/2. Esta observação proporcionou o impulso para que os inibidores de PARP1 fossem testados clinicamente, o que recentemente resultou na aprovação do primeiro inibidor, Olaparib, para o tratamento de pacientes com mutações hereditárias nos genes *BRCA*. Embora esta abordagem tenha mostrado bons resultados, têm sido identificados vários potenciais mecanismos de resistência. Para superar este problema, é necessário uma melhor compreensão da função molecular de BRCA1 e BRCA2 e das proteínas com as quais interagem. BRCA1 e BRCA2 desempenham um papel fundamental na decisão entre as vias de reparação de ADN, “DNA repair pathway choice”, e na resposta ao stresse durante a replicação, funções que estão relacionadas com a sensibilidade aos inibidores de PARP1. Os domínios BRCT de BRCA1 interagem com múltiplas proteínas e são necessários para a função supressora tumoral de BRCA1. Através deste domínio, BRCA1 forma três complexos mutuamente exclusivos com Abraxas, BRIP1 e CtIP, originando os complexos BRCA1-A, -B e -C, respetivamente. Neste estudo, decidimos investigar a importância dos complexos BRCA1-A e -B nesses dois mecanismos. No seu conjunto, estes resultados mostram que a depleção de Abraxas ou de BRIP1 e, conseqüentemente, a desagregação dos respetivos complexos, é sinteticamente letal com a inibição de PARP1. Aqui sugerimos que este fenótipo seja o resultado do papel desempenhado por BRCA1-A e BRCA1-B na reparação de ADN por recombinação homóloga, mais especificamente, na escolha da via de reparação do ADN. Além disso, a expressão de BRIP1, ou a formação de BRCA1-B, parece influenciar a expressão de Abraxas. Aqui, também propomos que os complexos BRCA1-A e -B desempenham funções na resposta ao stresse durante a replicação. No entanto, de forma a validar estes resultados, é necessária uma investigação mais aprofundada. De forma geral, estes resultados contribuem para uma compreensão completa das funções moleculares do BRCA1 e das proteínas com as quais forma complexos. A compreensão destas funções é crucial para entender os mecanismos de resistência aos tratamentos atuais usados em células com mutações nos genes *BRCA*, e para melhorar as abordagens terapêuticas correntes.

1. Introduction

1.1. DNA double-strand break repair pathway choice

Our genetic material is continuously challenged by genotoxic stress. DNA lesions arise from exogenous and endogenous sources, generating approximately 10^5 lesions per cell every day ¹. To ensure genome stability, cells have evolved the ability to sense DNA damage, activate the cell cycle checkpoint and initiate DNA repair. The crosstalk between both processes is known as the DNA damage response (DDR) and ensures that cell cycle progression is halted soon after DNA damage is detected, allowing the DNA repair machinery to repair the damage before cells continue with DNA replication and cell division ^{2,3}. In the case of persistent DNA damage, cells undergo either apoptosis or senescence ^{4,5}. Cells defective in DDR generally display heightened sensitivity towards DNA-damaging agents and many such defects cause human disease ¹.

Of all the lesions that can occur in the DNA, double-strand breaks (DSBs) are considered to be the most threatening form of DNA damage, as the integrity of both strands of the DNA duplex is compromised simultaneously ⁶. Failure to faithfully repair them can result in a variety of mutations, including chromosomal rearrangements that are characteristic of cancer cells. The repair of DSBs is achieved by two mechanistically distinct processes: non-homologous end joining (NHEJ), which promotes direct ligation of the two broken ends, and homologous recombination directed repair (HDR), which requires a homologous template to regenerate the region surrounding the break (Fig. 1). Homology searching, a central step of HDR, requires DNA 5' end resection. The decision to resect is critical to DSB repair pathway choice, wherein initiation of this process commits cells to HDR while preventing repair by NHEJ ^{7,8}. The choice between these two repair pathways depends on the phase of the cell cycle. NHEJ operates throughout the cell cycle but is particularly important in the G1 phase, since there is no template to perform HDR. To promote NHEJ, the protein complex formed by 53BP1 and RIF1 limits 5' end resection through recruitment of MAD2L2 ⁹⁻¹⁴. Inhibition of 5' end resection allows downstream factors to localize at DSBs that, ultimately, lead to ligation of the broken ends by DNA ligase IV ¹⁵. However, this happens in an error-prone manner, frequently resulting in small insertions, deletions, substitutions and translocations ¹⁵. On the other side, HDR is generally restricted to the S and G2 phases when DNA has replicated and the sister chromatid is available as a template. Hence, in S/G2, BRCA1 localizes at DSBs and, through its binding to CtIP,

promotes 5' end resection by opposing the inhibitory effect of the 53BP1 pathway^{10,16–18}. Then, BRCA2 promotes RAD51 nucleofilament formation, homology search, strand invasion, and replication of the genetic material⁸. This allows the repair to act in an error-free fashion, promoting genome stability through the precise repair of DNA double-strand breaks¹⁹. Therefore, depending on the cell cycle, cells must choose the appropriate pathway for DNA repair, NHEJ in G1 and HDR in S/G2. Failing to commit to the right choice endangers genomic integrity and can contribute to tumorigenesis.

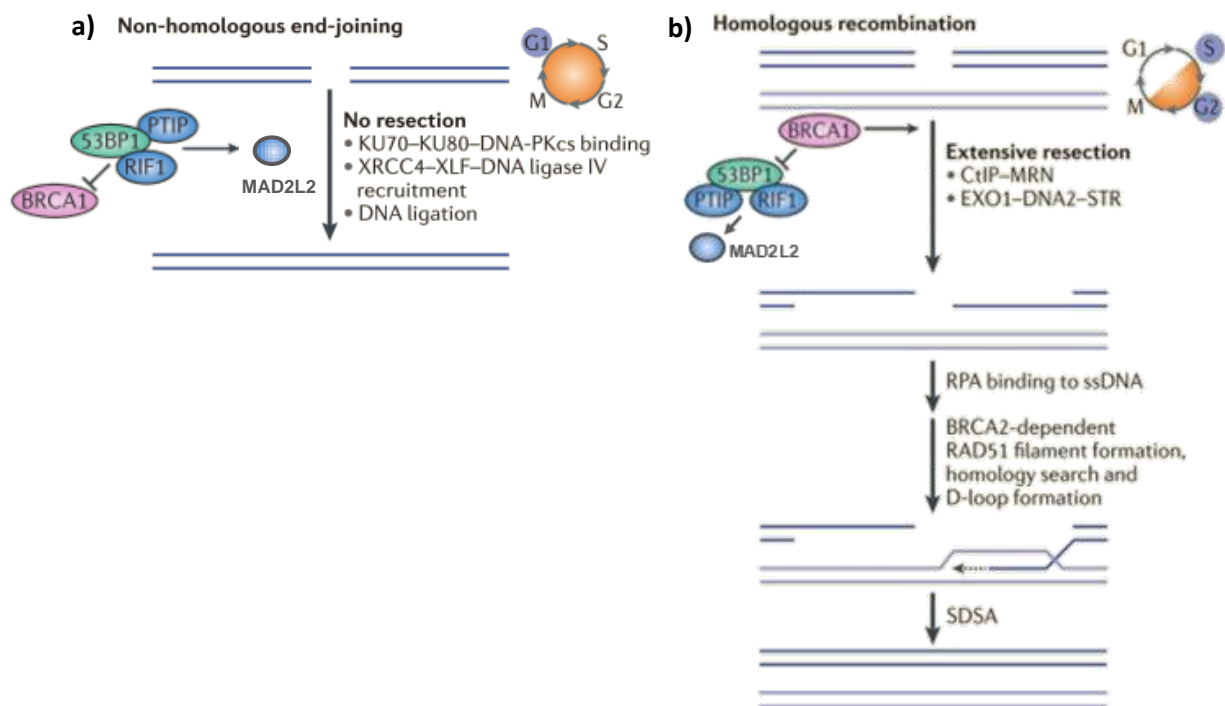


Figure 1- Repair of DSBs by NHEJ and by HDR. a) NHEJ operates throughout the cell cycle, being particularly important in G1. 53BP1 inhibits 5' end resection through the recruitment of RIF1 and the downstream protein MAD2L2, preventing the promotion of HDR by BRCA1 while committing to NHEJ repair. Inhibition of 5' end resection allows the KU70– KU80 complex, DNA-PKcs and the XRCC4–XLF–DNA ligase IV complex to localize at DSBs, leading to ligation of the broken ends by DNA ligase IV. b) HDR is restricted to the S and G2 phases of the cell cycle. It is initiated when BRCA1 is able to stimulate 5' end resection by releasing the inhibitory effect of 53BP1. CtIP then promotes 5' end resection through the interaction with the MRN complex and stimulation of its nuclease activity. End resection inhibits the binding of KU70–KU80 to DNA ends, thereby also inhibiting NHEJ. RPA rapidly coats the ssDNA generated by DNA end resection and is then replaced by the recombinase RAD51, a process dependent on BRCA2. RAD51 filament formation enables homology search, duplex invasion and DNA synthesis. Adapted from Panier and Durocher, 2013²⁰

1.2. Targeting Poly (ADP-ribose) polymerase (PARP) 1 in BRCA1 -deficient tumors

BRCA1, a key regulator of HDR, is a tumor suppressor gene, and germline mutations of the human gene account for most familial cases of breast and ovarian cancer. Cells with defects in *BRCA1* lack the ability to localize RAD51 to damaged DNA and, consequently, are unable to perform HDR. As a result, the error-prone NHEJ takes over, leading to an accumulation of genetic aberrations, which likely foster tumorigenesis. The genetic concept of synthetic lethality has been exploited as an approach to treat BRCA-deficient tumors. Synthetic lethality describes the situation in which defects in either one of two genes individually is compatible with cell viability, but when defects in the two are combined, lethality ensues (Fig. 2a) ^{21,22}. Inhibition of Poly (ADP-ribose) polymerase 1 (PARP1) has been shown to be synthetically lethal with deficiency of *BRCA1* ²³. PARP1 is an enzyme involved in DNA single-strand break (SSB) repair. Upon damage, PARP1 is recruited to the site of SSBs, where it binds the DNA and promotes DNA repair. PARP1 inhibition leads to accumulation of SSBs and to the stalling of the replication fork (RF) by trapping PARP1 on the DNA, which eventually leads to the collapse of the RF, causing DSBs (Fig. 2b). HDR is the preferred mechanism for repairing collapsed RFs. When *BRCA1* is dysfunctional, alternative DNA repair mechanisms such as NHEJ are used. These alternative processes sometimes fail to efficiently repair the replication fork, and this is ultimately deleterious to the cell. Thus, cells carrying *BRCA* mutations are up to 1,000 times more sensitive to PARP1 inhibition than wild-type cells. These observations provided the impetus for PARP inhibitors (PARPi) to be tested clinically, which recently led to the approval of the first PARPi, Olaparib, for the treatment of patients with germline mutations in *BRCA* genes.

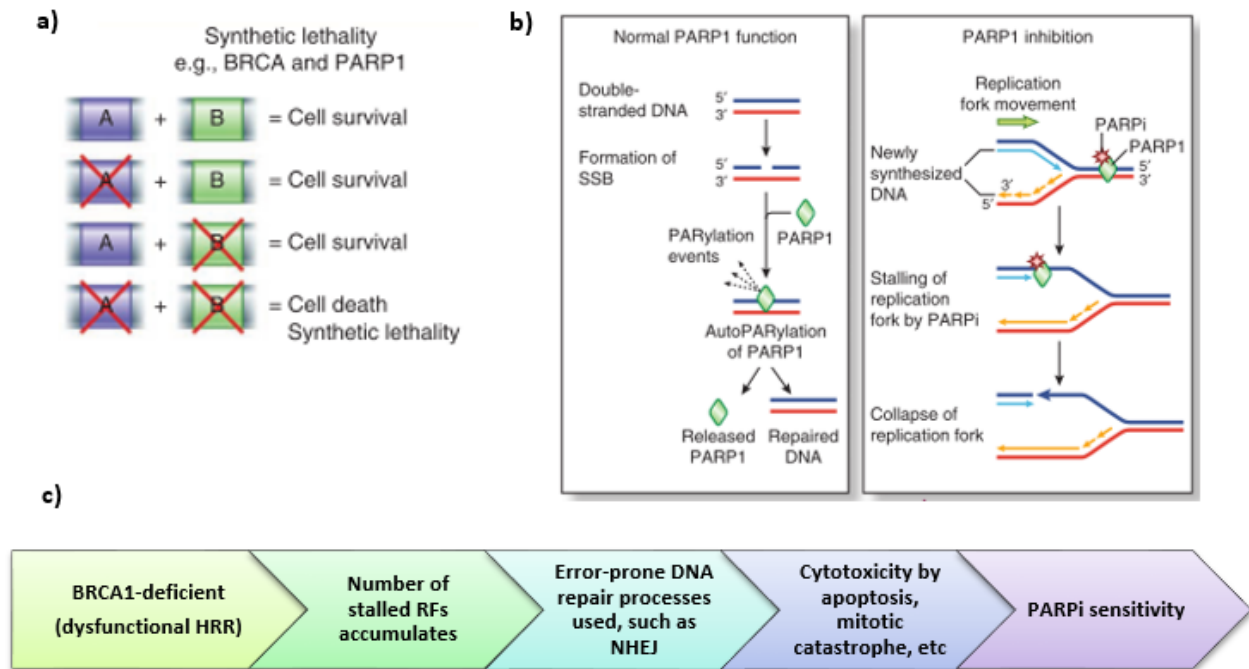


Figure 2 - Genetic concept of synthetic lethality and PARP1 inhibition in BRCA1-deficient cells. a) A genetic interaction in which single-gene defects are compatible with cell viability, but the combination of gene effects results in cell death. The first clinical exemplification of synthetic lethality in cancer was the targeting of BRCA-deficient tumor cells with PARPi. b) PARP1 is involved in the repair of SSBs. Upon damage, PARP1 is recruited to the site of SSBs, where it binds DNA and catalyses a series of PARylation events, promoting DNA repair. As part of this process, PARP1 autoPARylates, leading to its release from DNA. PARPi prevent the release of PARP1 from DNA, most likely by inhibiting autoPARylation. PARP1 autoPARylates, leading to its release from DNA. PARPi prevent release of PARP1 from DNA, most likely by inhibiting autoPARylation. PARP1 inhibition leads to the stalling of the replication fork by accumulation of SSBs, ultimately leading to the collapse of the RF, causing DSBs). c) Cells repair the RF preferably by HDR. Cells deficient in BRCA1 have a dysfunctional HDR and, therefore, the number of stalled RFs accumulates. Cells use alternative error-prone repair mechanisms, such as NHEJ, which are incapable of efficiently repairing the RF, resulting in chromosomal instability and subsequent cell death. This defect results in a hypersensitivity of BRCA1-deficient cells to PARPi. Adapted from Lord and Ashworth, 2013 ²¹.

1.3. Mechanisms of resistance to PARPi in BRCA1-deficient tumors

Although the use of PARPi in BRCA-deficient tumors has shown promise, emergence of drug resistance is a common clinical problem, affecting PARPi efficiency. Multiple potential resistance mechanisms have been identified. The most well-validated mechanism of resistance to PARPi seen in

patients with *BRCA1* mutations is genetic reactivation of *BRCA1*-mutated alleles which can occur because of alternative splicing, retromutations, or secondary mutations restoring *BRCA1*'s reading frame. It was also shown that transcription of silenced *BRCA1* alleles can be restored upon promoter demethylation or gene fusions to distant promoters^{24–26}. Alternatively, resistance to inhibition of PARP1 can also result from *BRCA1*-independent restoration of HDR. The most well-studied and validated mechanism was the finding that loss of 53BP1 rescues the HDR deficiency, proliferation defect and PARPi hypersensitivity of *BRCA1*-deficient cells^{27,28}. 53BP1 deletion allows the resection of broken DNA ends, leading to error-free repair by HDR. These findings led to novel mechanistic insights in DSB repair and to date loss of several downstream effector proteins of 53BP1 have been shown to render *BRCA1*-deficient cells resistant to PARPi, including MAD2L2^{13,14}, RIF1^{10,11}, PTIP¹², Artemis²⁹. Besides, recently it was shown that *BRCA1*-mutant tumors may also acquire PARPi resistance by amplification of *TIRR*, involved in the regulation of 53BP1, leading to overexpression of *TIRR*, which results in impaired function of 53BP1 and, subsequently, in HDR restoration³⁰. These findings reveal that the DNA damage response pathway can be rewired to restore HDR. Independent of HDR, recent studies have shown that *BRCA1* has DSB-independent functions during replication stress and it has been proposed that resistance to PARPi might also occur due to protection of RF³¹. However, many other mechanisms of resistance are yet to be found. A better understanding of how *BRCA1* contributes to DNA damage and replication stress pathways will help clarify how *BRCA1*-deficient tumors can acquire resistance to PARP1 inhibitors and, eventually, can help to find new therapeutic targets.

1.4. *BRCA1*: a master regulator of genome integrity

BRCA1 is intimately involved in diverse cellular processes that ensure genome stability and promote cell survival. Through its ability to associate with multiple proteins, *BRCA1* has important roles in the DNA damage response, including cell cycle checkpoint control and DNA repair. Moreover, recent reports also demonstrate a new role of *BRCA1* in the replication stress response^{31–34}. *BRCA1*, which is located on chromosome 17q21, is a large protein of 1,863 amino acids. It harbors two important highly conserved domains at each end of the protein, an amino-terminal RING domain and two BRCT domains at its carboxyl terminus. The fact that these domains are frequently targeted by many clinically important mutations indicates that they are essential for *BRCA1* function^{35–37}. The

RING domain is required for heterodimerization of BRCA1 with BARD1. BRCA1-BARD1 heterodimerization is required for their stability in vivo and for their nuclear localization^{38,39}. This heterodimer has E3 ubiquitin ligase activity and BRCA1/BARD1-dependent ubiquitin conjugates occur at sites of DNA DSBs suggesting that the BRCA1-BARD1 heterodimer is important for DNA repair and, therefore, is important for the tumor suppressor activity of BRCA1⁴⁰. On the other hand, the BRCA1 BRCT domains are conserved in multiple DDR proteins domains and are thought to be integral to BRCA1's ability to regulate a diverse set of cellular processes that confer its tumor-suppressing activity. The paired BRCT domains form a binding site that recognizes a phospho-SPxF (S, serine; P, proline; x varies; F, phenylalanine) motif and mediates the association of BRCA1 to phosphorylated proteins Abraxas, BRIP1 and CtIP. Cell cycle-dependent phosphorylation of these proteins at the serine residue of their p-SPxF motif by CDK is required for BRCA1 interaction. Since, these proteins associate with the same binding site of BRCA1, they form three mutually exclusive different complexes known as BRCA1-A (Abraxas), -B (BRIP1) and -C (CtIP) (Fig. 3). Although it remains elusive how these complexes are involved in BRCA1 signaling, it appears that these three complexes partially undertake BRCA1's role in cell cycle checkpoint and in DNA repair, that maintain genome stability and, thus, may be essential for the tumor suppression function of BRCA1. Of the three BRCA1-forming complexes, BRCA1-C is the only one known to actively participate in HDR, as it is required for the fine-tuning of DNA end resection^{10,41,42}. Besides, loss of CtIP has been shown to render cells sensitive to PARP inhibition⁴³. On the contrary, the exact role of BRCA1-A and -B in HDR still requires further study.

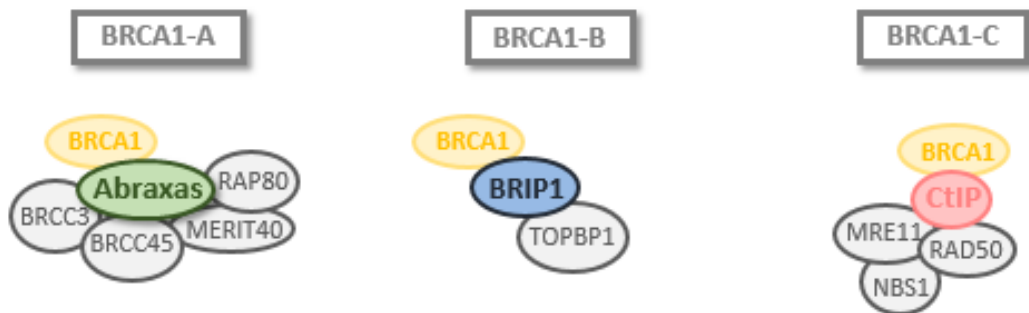


Figure 3 – BRCA1 Complexes. BRCA1-A complex is composed of BRCA1, RAP80, Abraxas, MERIT40, BRCC45, and BRCC36. BRCA1-B is composed of BRCA1, TopBP1, and BRIP1. BRCA1-C comprises BRCA1, CtIP and MRE11–RAD50–NBS1 complex (MRN complex).

1.5. Roles of BRCA1-A and -B complexes

The BRCA1-A complex is composed by the ubiquitin interacting motif (UIM) containing protein RAP80, adapter protein Abraxas, the scaffolding proteins MERIT40 and BRCC45, and the deubiquitinating enzyme (DUB) BRCC36³⁷. The phosphorylation of the C-terminal serine (p-S406) of the SPxF motif of Abraxas is responsible for the interaction with the BRCT domain of BRCA1⁴⁴. Abraxas acts as a central adapter linking BRCA1 to other components in the BRCA1-A complex and it was demonstrated to play a role in tumor suppression⁴⁵. BRCA1 is targeted to DSBs sites through its association with the A complex, which in turn localizes at DSBs through the UIMs of RAP80, which recognize the Lys⁶³ poly-ubiquitin chains of the histone H2AX^{44,46}. This process is initiated by ATM-mediated H2AX phosphorylation near the DNA lesions and is required for the DDR. Additionally, BRCA1-A has been shown to be required for preventing over-resection of DSB ends, a process dependent on the Lys⁶³-deubiquitinating function of the enzyme BRCC36⁴⁷⁻⁴⁹. The BRCA1-A complex is also involved in the G2/M checkpoint in response to ionizing radiation (IR)-induced DNA damage, whereas BRCA1-B seems to be necessary for the S-phase checkpoint in response to replication stress⁵⁰⁻⁵². BRCA1-B is composed by the helicase BRIP1 and by TOPBP1. The interaction of BRIP1 with BRCA1 requires the phosphorylation of its C-terminal serine (p-S990) of its SPxF motif⁵³. Defects in BRIP1 lead to reduced HDR and delayed DNA repair⁵⁴. Binding of BRIP1 to TOPBP1 is important for proper replication, being a requirement for replication checkpoint control, as it mediates activation of ATR-dependent phosphorylation events in response to replication stress. Furthermore, it was suggested that a specific interaction between TOPBP1 and BRIP1 is likely to be required for the extension of ssDNA regions and RPA loading following replication stress⁵². As a member of the Fanconi anemia (FA) proteins, BRIP1 (also known as FANCI) also plays a role in DNA interstrand crosslink (ICL) repair⁵⁵. Moreover, it was shown that loss of BRCA1-BRIP1 interaction promotes a switch from HDR to pol η -dependent bypass⁵⁶.

Consistent with the hypothesis that Abraxas and BRIP1 contribute to BRCA1's role in tumor suppression, both have been associated with breast and ovarian cancer^{45,54,57-60}. Thus, clarifying the diverse functions of BRCA1-A and BRCA1-B, besides helping understanding the molecular function of BRCA1, its binding partners and the involved molecular pathways, can result in a meaningful impact on disease treatment.

2. Objectives

2.1. Main Objective

Understand the role of BRCA1-A and -B complexes in DNA repair pathway choice and in replication stress.

2.2. Specific Objectives

- Disruption of BRCA1-A and -B complexes using the CRISPR-Cas9 system to generate knockout single clones of *ABRAXAS* and *BRIP1*.
- Test sensitivity of knockout clones to PARPi (Olaparib) by long term clonogenic assays.
- Analysis of the effect of the disruption of BRCA1-A and -B complexes on DNA repair pathway choice.
- Analysis of replication stress markers in knockout clones.

3. Materials and Methods

3.1. Cell culture and clonogenic survival assays

For this study, two cell lines were used: HeLa and HEK293T. HeLa cells are derived from cervical cancer cells. HEK293T cells are derived from human embryonic kidneys and are transformed with large T antigen. All cell lines were maintained in DMEM with 100U penicillin, 0.1 mg/ml streptomycin, 2mM L-glutamine and 10% fetal bovine serum. All cells were maintained in a 5% CO₂ incubator at 37°C.

For clonogenic assays, cells were seeded in 6cm dish at density of 20,000 per dish in the presence of PARPi (Olaparib, 1 or 3µM) or DMSO. Medium was refreshed every 5 days. After 12 days, plates were fixed with 10% formalin and stained with a 0.1% (w/v) crystal violet solution. Colony quantification was performed by crystal violet extraction with 10% (v/v) acetic acid and absorbance (590nm) was measured.

3.2. Cloning and CRISPR–Cas9 genome editing

CRISPR guides were designed using online tool *Benchling* (<https://benchling.com>). The sequence of the single guides (sgRNA) used for the generation of knockouts are: Abraxas KO clone #9-1: 5'- GAGGGGGAGAGTACGTCGG - 3'; Abraxas KO clone #14-2: 5'- CCTCAACACGGACTCGGACA - 3'; BRIP KO clone #7-3 and #8-7: 5'- TCTGAATATACAATTGGTG- 3'. In order to clone the guide sequence into the sgRNA, the oligos were synthesized in the form: 5' – CACCGNNNNNNNNNNNNNNNNNNNNNN – 3' and the reverse complement 5' – AAACNNNNNNNNNNNNNNNNNNNNNNC – 3'. The cloning was based on the approach developed by the Yamamoto lab ⁶¹. To anneal the oligos, 1 µl of each oligo (100µM) was added to 8 µl water, incubated at 95°C for 5 minutes and left at room temperature for 1h. Afterwards, 1.5 µl of vector pX330-U6-Chimeric_BB-CBh-hSpCas9 ⁶² (25ng/µl) (Addgene plasmid # 42230) were added to 2.5 µl of annealed oligos (10 µM), 0.5 µl of the restriction enzyme BbsI (NEB), 0.5µl of Quick ligase (NEB), 1µl of 10x T4 DNA ligase buffer (NEB), and 4 µl of water were mixed and incubated at 37°C for 5min followed by 10 min at 16°C. This cycle was repeated three times. In order to perform an extra digestion to ensure complete digestion of the empty plasmid, 0.5 µl of BbsI and 1

μ l of 10X Buffer G (Thermo Fisher Scientific) were mixed and incubated at 37°C for 1h followed by an incubation at 80°C for 5min. Next, 2 μ l of the cloning product were added to 25 μ l of competent cells XL10-Gold (Agilent Technologies) and transformed using heat shock. After incubation in S.O.C. medium (Thermo Fisher Scientific) at 37°C during 1h, cells were plated in LB agar plates with 100 μ g/mL ampicillin and incubated overnight at 37°C. On the next day, 8 colonies per sgRNA were picked and the plasmids were isolated using the QIAprep Spin Miniprep Kit (QUIAGEN) as suggested by the manufacturer. The sgRNA insertion was accessed by Sanger sequencing.

For generation of knockout clones, HeLa cells were plated in 6-well plates at a density of 150,000 cells per well. The next day cells were co-transfected with 3 μ g of the plasmid containing the sgRNA and Cas9 and with 1 μ g of the donor plasmid. After 3 days, medium was changed and Blasticidin (10 μ g/ml) was added. 10 days after addition of selection, resistant colonies were isolated (one colony per well) and expanded. Genomic DNA was isolated, and cells lysates were used for protein analysis.

3.3. shRNA-mediated silencing

Glycerol stocks containing hairpins were obtained from MISSION shRNA library (Sigma, TRC) clones. Plasmid DNA isolation was carried out with the HiPure Plasmid Midiprep Kit (Invitrogen), as suggested by the manufacturer. HeLa cells were transduced with the following pLKO-puro or pLKO-blast shRNA lentiviral particles: 53BP1: 5' -GATACTTGGTCTTACTGGTTT- 3'; RIF1: 5'-CGCATTCTGCTGTTGTTGATT-3'; MAD2L2: 5'-CCGGAGCTGAATCAGTATAT-3'; BRCA1: 5'-GCCCCACCTAATTGTACTGAAT -3'.

3.4. Transfections and lentiviral infections

For generation of knockout clones, we used the TransIT®-LT1 transfection reagent (Mirus) and we followed the manufacturer's protocol with slight changes: we used a ratio of 2:1, i.e., 6 μ l of TransIT®-LT1 transfection reagent to 3 μ g of plasmid. Cells were cultured in DMEM as described in 3.1.

For generation of lentiviral particles we seeded HEK293T cells at a density of 4,000,000 cells per 10cm dish. The following day, HEK293T cells were transfected as follows: a mix containing the lentiviral packaging vectors (pVSVG – 3.5 μ g, pRRE – 6.5 μ g and pREV – 2.5 μ g), the pLKO-puro or

pLKO-blast shRNA-containing vector (10 µg) and 0.25M of CaCl₂ in MilliQ water was prepared in a volume of 500 µL, to which 500 µL of 2xHBS (280 mM NaCl, 1.5 mM Na₂PO₄·7H₂O, 50 mM HEPES; pH 7) was added dropwise, while vortexing at maximum speed, and immediately added to the cells. Culture medium was refreshed 16h before refreshing the culture medium. 32h post transfection, lentiviral particles were obtained by filtering the supernatant of 293T cells. For lentiviral transduction, HeLa cells were seeded at a density of 200,000 per well in 6-well plates. After 24h, cells were transduced with shRNA-containing lentivirus. In order to increase transduction efficiency, polybrene was added to the cells in a final concentration of 8µg/ml. 16h post infection, medium was refreshed and cells selection was added (Puromycin (2µg/ml) or Blasticidin (10µg/ml)). Cells were cultured in DMEM as described in 3.1.

3.5. DNA extraction and PCR

Genomic DNA from CRISPR-ca9 single clones was isolated using DNeasy Blood & Tissue Kits (QUIAGEN), as suggested by the manufacturer. For analysis of blasticidin resistance cassette insertion, Phusion High-Fidelity DNA Polymerase kit (Thermo Fisher Scientific) was used. For analysis of insertion into *ABRAXAS* gene, the following set of primers were used: Fw 5'-CCTGTCAACCGTGTTTCATTTTGATAGC3' and Rv 5'-GCCCAAGTTTCCACAGCTACAG-3'. For analysis of insertion into *Brip1* gene, the following set of primers were used: Fw 5'-ACGGAGTTGTAGAGAGAGAG-3' and Rv 5'-AGTAGTTTCCAGAGGTTAGA-3'. PCR product analysis was performed by agarose gel (1% w/v) electrophoresis.

3.6. Protein extraction and Western Blot

Cells were seeded at a density of a 1,000,000 cells in a 6cm dish. Whole-cell lysates were prepared by scraping cells in 2x SDS sample buffer. Protein concentration was determined for each sample using the standard BCA protein assay (Pierce). Protein concentrations were normalized to the least concentrated sample, and samples were separated on precast 4-12% Bis-Tris gels (Invitrogen). Proteins were then transferred on to nitrocellulose blotting membranes (GE Healthcare) and blocked in 5% milk, or 5% BSA solutions in 0.1% PBS-Tween20. Primary antibodies were diluted in 1% milk or

5% BSA solutions in 0.1% PBS-Tween20 and incubated overnight at 4°C. Membranes were washed three times with 0.1% PBS-Tween20 and incubated with secondary antibodies for 1h at room temperature. Western blotting was performed using horseradish peroxidase (HRP)-conjugated secondary antibodies (1:7000), which were detected by enhanced chemiluminescence (ECL) (Thermo Fisher Scientific). Blots were developed using Amersham Hyperfilm ECL films (GE Healthcare). Primary antibodies used: Abraxas (A302-181A, Bethyl, 1:1000); BRIP1 (ab151509, Abcam, 1:1000); BRCA1 (sc-6954, Santa Cruz, 1:200); 53BP1 (A300-272A, Bethyl, 1:2000); CtIP (22838, Santa Cruz, 1:500); MAD2B (135977, Santa Cruz, 1:200); Histone H2B (07-371, Millipore, 1:2000); Histone H3 (ab1791, Abcam, 1:10000). Histones H3 and H2B were blotted as loading controls.

3.7. Immunofluorescence

Cells were seeded on 8-well chamber slides (Millipore) and allowed to adhere. In order to visualize DDR foci, cells were irradiated with 5 Gy and fixed after 3h. For replication stress experiments: to visualize γ -H2AX staining, cells were fixed after 3h of treatment with hydroxyurea (HU) (2mM); for staining with Bromodeoxyuridine (BrdU), cells were cultured with BrdU-containing medium (10 μ g/ml) for 30h, and then released in new medium with HU (2mM) and fixed after 3h of treatment. For BrdU staining, cells were washed with 0.5% Triton/PBS for 3min before fixation. Cells were fixed in 4% paraformaldehyde/PBS, for 10 min. Cells were permeabilized for 10 min in 0.5% Triton/PBS and incubated for 1h with blocking solution (0.02% Triton, 5% NGS, 5% FCS in PBS). Primary antibodies were diluted in blocking solution and incubated overnight at 4°C. The following day, cells were washed three times with 0.02% Triton/PBS and incubated with fluorophore-conjugated secondary antibodies (Alexa Fluor 488 anti-rabbit IgG; Alexa Fluor 568 anti-mouse IgG; Invitrogen), diluted 1:500 in blocking solution, for 1h at RT. After three washes with 0.02% Triton/PBS, slides were mounted in Vectashield (Vector Laboratories) containing DAPI. Fluorescence images were obtained on a Leica SP5 confocal system equipped with Ar, Kr and HeNe lasers. Images were acquired using a 63 \times , 1.32 NA oil immersion objective (Leica), and processed with LAS-AF software. Primary antibodies used: 53BP1 (A300-272A, Bethyl, 1:2000); Cyclin A (MS-1061-S0, Thermo Fisher Scientific, 1:500); Cyclin A (sc-751, Santa Cruz, 1:100); RIF1 (A300-569A, Bethyl, 1:1000); γ -H2AX (Ser 139) (5636, Millipore, 1:500); BrdU (NA61, Calbiochem, 1:50); CENPF (SAB2702181, Sigma, 1:500)

4. Results

4.1. Generation of knockout clones of *ABRAXAS* and *BRIP1*

Abraxas and BRIP1 are the central adapters of the BRCA1-A and -B complexes, respectively. In order to investigate the role of BRCA1-A and -B complexes in DNA repair pathway choice and in replication stress, we used the CRISPR-Cas9 system to generate Abraxas and BRIP1 knockout (KO) clones in HeLa cells, in order to be used as tools for this study. Previously, Lackner and colleagues described a strategy that enables the tagging of endogenous loci using the CRISPR-cas9 system and one generic donor plasmid⁶³. The donor plasmid contains a tag of interest which is flanked by two sgRNA cleavage sites that correspond to a genomic locus in Zebrafish (*tia1l*) that is absent in human cells. The donor plasmid also encodes a U6 promoter driving the expression of the *tia1l* sgRNA. When cells are transfected with Cas9, the donor plasmid and a sgRNA specific to the region of the gene where the tag should be incorporated, the tag is released from the plasmid and subsequently integrated into the gene of interest by NHEJ. To obtain our knockout clones, we made use of this approach by using the donor plasmid with a Blasticidin resistance (Blast^R) cassette as a tag (Fig.4a). Co-transfection of the donor plasmid with a cas9-expressing plasmid⁶², in which we cloned a sgRNA, allowed us to use Blasticidin to select the clones where the plasmid was integrated. As a negative control, we transfected HeLa cells with donor plasmid and with the cas9-expressing plasmid, without sgRNA cloned. We design 3 sgRNA per gene, however, only 2 of the sgRNAs targeting *ABRAXAS* and 1 sgRNA targeting *BRIP1* efficiently generated Blasticidin-resistant colonies. The resistant colonies were isolated and screened using western blot and PCR (Fig.4b,c,d). After analysis, two clones per gene were selected (*Abraxas* KO # 9-1 and # 14-2; *BRIP1* KO # 7-3 and # 8-7) and used as tools for the following experiments.

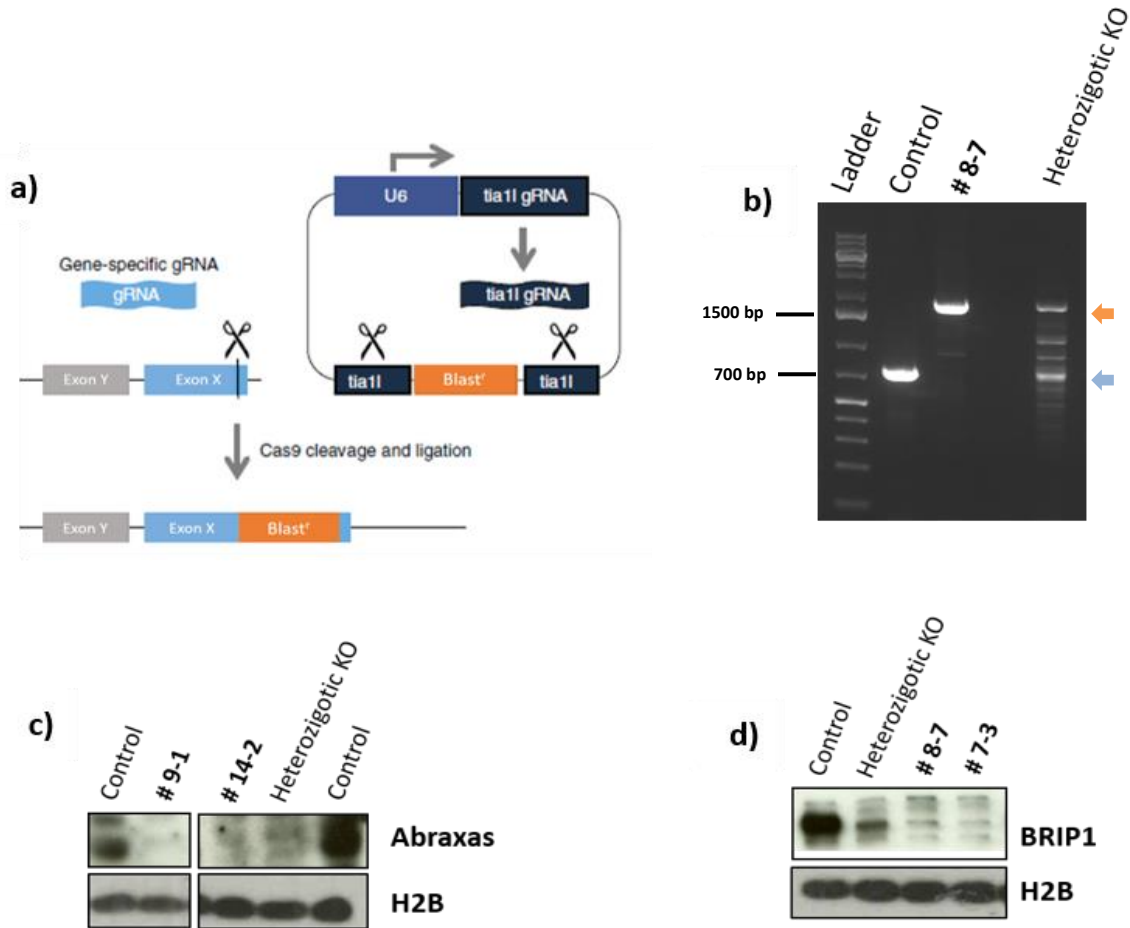


Figure 4 – Identification of Abraxas and BRIP1 knockout clones in HeLa cells. a) Schematic representation of our CRISPR-Cas9 approach. Adapted from Lackner *et al.* 2015⁶³. b) Exemplification of how a PCR followed by agarose gel electrophoresis can identify knockout clones. For comparison, PCR products from a control, a knockout (BRIP1 KO # 8-7), and heterozygous sample are shown. Blue arrow indicates the size of the fragments without tag insertion, and orange arrow indicates the size of the fragments with tag insertion. Samples that only display a band, corresponding to the upper fragment (with insertion of tag), have the targeting gene disrupted. Samples that exhibit both fragments don't have tag insertion in all alleles and, thus, were considered to be heterozygous and discarded. c), d) Western-blot analysis representing protein expression of knockout clones of Abraxas and BRIP1, respectively. For comparison, samples from a control, knockout and heterozygous clones are shown. Histone H2B was blotted as a loading control.

4.2. Sensitivity of knockout clones to Olaparib

BRCA1 dysfunction, results in cells markedly sensitized to inhibition of PARP1 enzymatic activity. Hence, we decided to test if our knockout clones, where the BRCA1-binding complexes A and B are disrupted, are also sensitive to PARP1 inhibition. Cells were treated for 12 days with 1 μ M

Olaparib. As positive control, cells transduced with shBRCA1 lentiviral particles were also treated. As expected, while untransduced cells don't show sensitivity to Olaparib, cells transduced with shBRCA1 show toxicity to the drug (Fig.5). On the other hand, both Abraxas and BRIP1 knockout clones were sensitive to Olaparib, although not as sensitive as the cells transduced with shBRCA1 lentiviral particles (Fig.5). These results suggest that Abraxas and BRIP1 and, therefore, their respective complexes (BRCA1-A and -B, respectively), might be important for HDR.

Tumor cells are known to have the ability to adapt upon stress, overcome cell death, and to become drug-resistant. As HeLa cells are a tumor-derived cell line, we expected cells to easily adapt to knockout of Abraxas and BRIP1. Therefore, as the experiments in this study were performed in different time-points, in each of the following chapters we display a clonogenic assay as control, which was performed in parallel with the respective experiments, where sensitivity to Olaparib can be used as a read-out of adaptation of cells to the stress generated by depletion of these proteins.

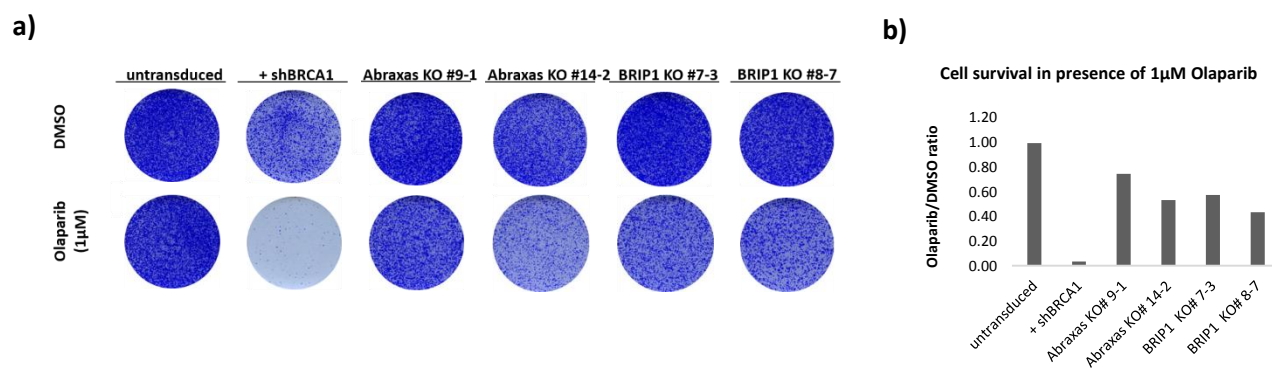


Figure 5 – Sensitivity to Olaparib. a) Crystal violet staining of untransduced HeLa cells, HeLa cells transduced with shBRCA1 lentivirus particles, and Abraxas and BRIP1 knockout clones treated with DMSO (vehicle) or Olaparib (1µM) during 12 days. b) Quantification of cell survival from a) by measurement of extracted crystal violet absorbance at 590 nm. Graph shows cell survival ratio between Olaparib and DMSO treatment. All values were normalized by the mean of the blank. Mean is shown from three independent measurements.

4.3. Analysis of the DNA repair pathway choice upon Abraxas and BRIP1 depletion

Since depletion of Abraxas and BRIP1 appears to be important for HDR, we investigated if these proteins play a role in pathway choice. In S/G2 phases of the cell cycle, when BRCA1 is depleted, 53BP1 and downstream factors are no longer suppressed, allowing their localization at

DSBs sites. Therefore, NHEJ repair can takeover. In order to investigate if BRCA1-A and –B complexes are involved in DNA repair pathway choice, we analyzed nuclear foci formation of 53BP1 and the downstream factor RIF1 in S/G2 phases of the cell cycle, after induced DNA damage by ionizing radiation (5 grey (Gy)). Untransduced HeLa cells, cells transduced with shBRCA1 lentivirus, and two Abraxas and BRIP1 knockout clones irradiated and non-irradiated were fixed after 3 hours and 53BP1 and RIF1 foci formation was analyzed by immunofluorescence (IF). Cells were co-stained for CENPF. CENPF is a kinetochore protein and was used as a cell cycle marker as its expression is induced at G1/S, increases during S phase until it peaks at G2 and starts to be degraded at mitosis⁶⁴. In order to distinguish between G1 and S/G2 cells, the mean fluorescence intensity (MFI) of CENPF was quantified for all the cells and a threshold was set. Hence, low CENPF expressing cells were considered to be in G1 and high CENPF expressing cells in S/G2. Generally, 53BP1 and RIF1 formed less foci in high CENPF cells when compared with low CENPF cells, as could be expected due to the opposition imposed by BRCA1 during S/G2 (Fig.6c, d). Upon knockdown of BRCA1, cells showed increased 53BP1 and RIF1 foci formation during S/G2, when compared to the parental untransduced cells (Wt), as it was expected (Fig.6). Abraxas knockout clones both showed increased 53BP1 foci formation (Fig.6a,c), however, only the clone #14-2 showed a significant increase of RIF1 foci in S/G2 (Fig.6b,d). On the other hand, only BRIP1 clone #8-7 showed significant increase of 53BP1 foci (Fig.6a,c), whereas both clones showed increase of RIF1 foci in S/G2 (Fig.b,d).

Looking at the control clonogenic assay (as explained in the previous section, 4.2.), cells transduced with shBRCA1 showed increased toxicity, when compared with untransduced Wt, as expected (Fig.7). Moreover, all the knockout clones displayed sensitivity to the inhibition of PARP1, although not to the same extent as cells with BRCA1 knockdown, with the exception of the Abraxas knockout clone #14-2, which appears to be as sensitive as cells transduced with shBRCA1 (Fig.7). This corroborates with the observation that the clone also has similar or higher levels of 53BP1 foci than cells with BRCA1 knockdown. However, the same doesn't happen with RIF1 foci formation. Although the results obtain from analysis of foci formation were not completely reproducible between 53BP1 and RIF1, in general, the number of foci in S/G2 increased in both experiments, which might indicate that BRCA1-A and –B complexes are involved in DNA repair pathway choice.

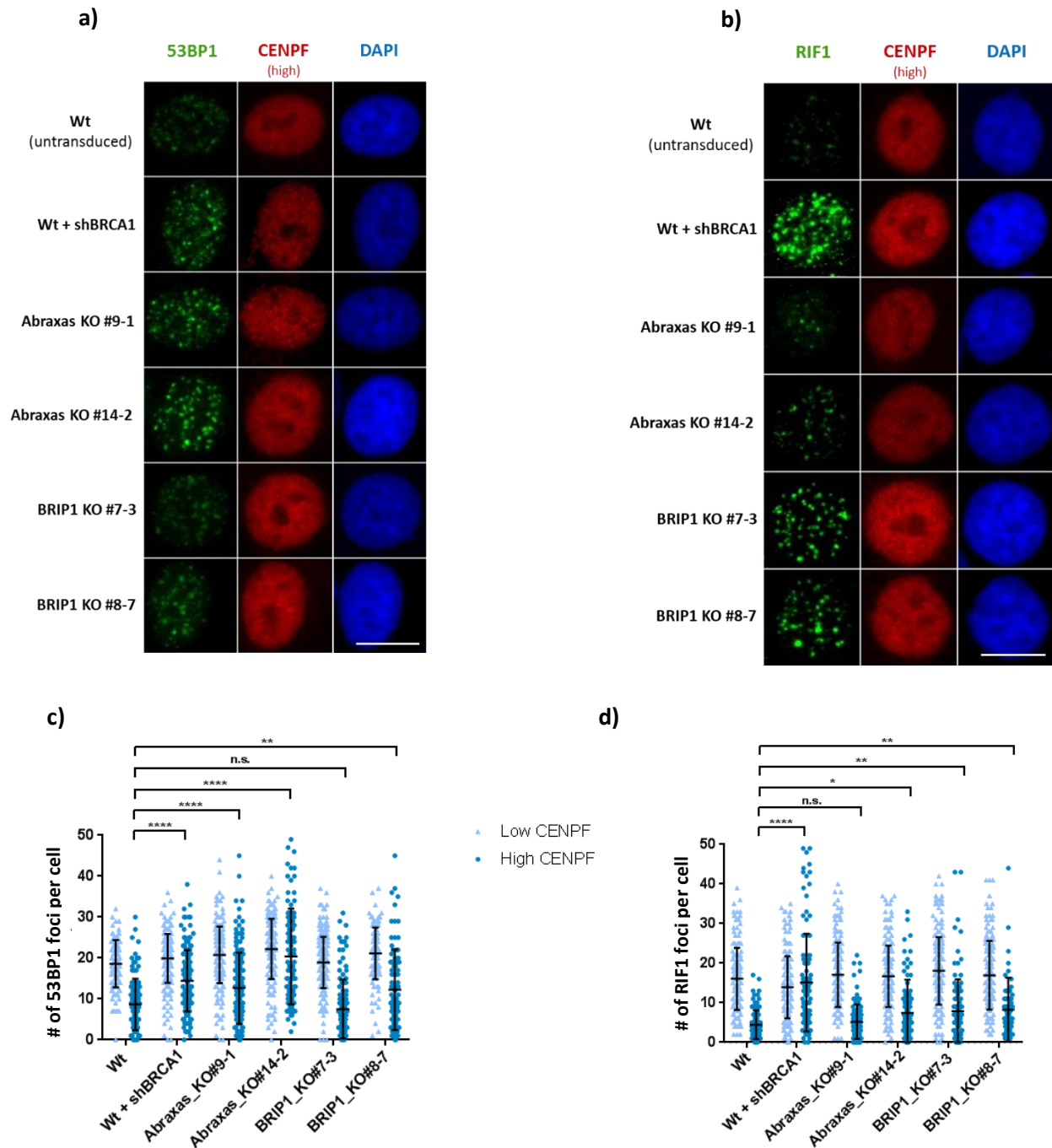


Figure 6 – 53BP1 and RIF1 foci formation. a) Representative images of 53BP1 and b) RIF1 nuclear foci in the indicated cells, 3h after exposure to ionizing radiation (5 Gy), visualized by immunofluorescence. The cells shown were considered to express high CENPF indicating to be in the S/G2 of the cell cycle. Scale bar: 14µm. c) Quantification of 53BP1 and d) RIF1 foci in more than 100 cells exposed to 5 Gy, per condition. Each dot represents one cell (n=1; mean ± s.d.). Statistical analysis was performed in GraphPad Prism 7 using a two-way ANOVA test. Results from statistical analysis of “High CENPF” group are displayed in the graphic. n.s., not significant; *, P < 0.05; **, P < 0.01; ****, P < 0.0001.

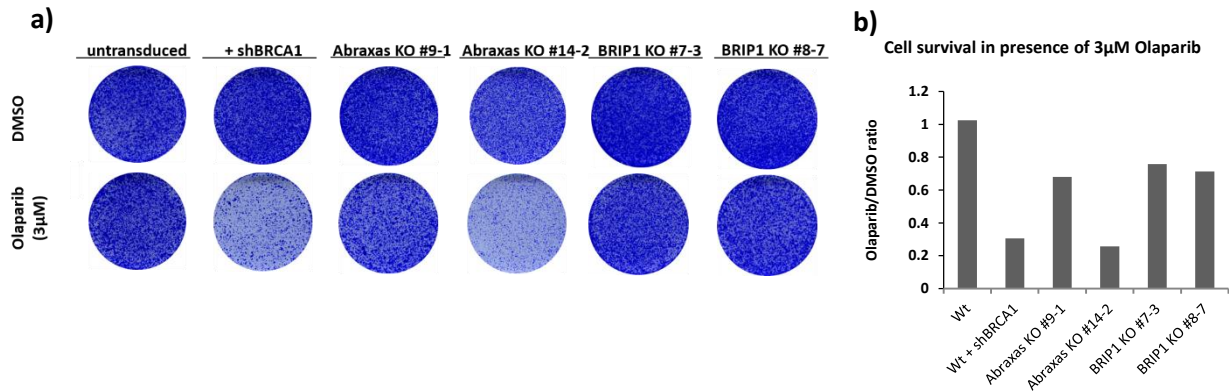


Figure 7- Clonogenic assay in the presence of 3µM Olaparib at the time of experiments from Fig.6. a) Crystal violet staining of untransduced HeLa cells, HeLa cells transduced with shBRCA1 lentivirus particles, and Abraxas and BRIP1 knockout clones clones treated with DMSO (vehicle) or Olaparib (3µM) during 12 days. b) Quantification of cell survival from a) by measurement of absorbance extracted crystal violet at 590 nm. Graph shows cell survival ratio between Olaparib and DMSO treatment. All values were normalized by the mean of the blank. Mean is shown from three independent measurements.

As referred to previously, restoration of HDR is a mechanism by which BRCA1-deficient tumor cells can acquire resistance to PARP1 inhibitors. One of the best studied factors that leads to HDR restoration, and resistance of these cells to PARP1 inhibition, is 53BP1 loss^{27,28}. Because knocking out Abraxas and BRIP1 appears to lead to sensitivity to PARP1 inhibition, and because depletion of these proteins leads to increase of 53BP1 and RIF1 foci formation upon DNA damage, as occurs in BRCA1-deficient cells, we decided to investigate if depletion of 53BP1 would also rescue the toxicity of PARP1 inhibition in the Abraxas and BRIP1 knockout clones. To this end, we silenced 53BP1 with shRNA in WT mother, in cells transduced with shBRCA1 and in the two Abraxas and BRIP1 knockout clones and performed a clonogenic survival assay and analyzed protein levels by Western Blot. Unfortunately, single knockdown of 53BP1 led to some degree of lethality, and co-knockdown of both BRCA1 and 53BP1 didn't rescue the lethality of BRCA1-knockdown cells to Olaparib, opposite to what was expected (Fig.8a,b). On the other hand, knockdown of 53BP1 in Abraxas knockout clones led to the rescue of one of the two clones (KO #9-1), and both BRIP1 clones (Fig.8a,b). Contrarily, knockdown of 53BP1 in Abraxas knockout #14-2 led to higher toxicity in Olaparib (Fig.8a,b). Moreover, 53BP1 knockdown appears to lead to slightly impaired growth in knockout clones, which is revealed by the diminished number of cell colonies upon treatment with the vehicle, when compared with the corresponding untransduced clones in the same condition. Furthermore, analysis of protein levels, revealed a decrease in Abraxas in cells transduced only with sh53BP1, co-transduced with sh53BP1 and shBRCA1. The same reduction in Abraxas protein levels was observed in BRIP1 knockout

clones, both untransduced and transduced with sh53BP1, when compared with untransduced (Wt) mother cells or with BRCA1 knockdown cells (Fig.8c). Oppositely, BRIP1 protein levels didn't change in any of the other conditions (Fig.8c). Protein expression levels of CtIP, another BRCA1-forming complex protein (BRCA1-C), involved in the fine-tuning of DNA end resection^{10,41,42}, was also analyzed. CtIP expression levels increased in cells transduced only with sh53BP1, co-transduced with sh53BP1 and shBRCA1, and in Abraxas and BRIP1 knockout clones, both untransduced and transduced with sh53BP1, when compared with untransduced (Wt) mother cells or with BRCA1 knockdown cells (Fig.8c).

Since, in contrast to literature, knockdown of 53BP1 didn't rescue the lethality of PARP1 inhibition in BRCA1 knockdown cells, we decided to repeat the experiment with cells transduced with shMAD2L2. MAD2L2, is a downstream partner of 53BP1, involved in the suppression of 5'-end resection, and its loss in BRCA1-deficient tumor cells was shown to lead to resistance to PARP1 inhibitors^{13,14}. Knockdown of MAD2L2 led to slight impaired growth in cells co-transduced with shBRCA1 and shMAD2L2 and in knockout clones, which is revealed by the diminished number of cell colonies upon treatment with the vehicle, when compared with the corresponding untransduced clones in the same condition, as shown in the clonogenic assay (Fig.9a,b). Single knockdown of MAD2L2 doesn't lead to lethality, and co-knockdown of both BRCA1 and MAD2L2 did rescue the lethality of BRCA1-knockdown cells to Olaparib, consistent with the literature (fig.9a,b). Additionally, knockdown of MAD2L2 rescued the lethality of PARP1 inhibition in the two clones of both Abraxas and BRIP1 knockout cells (Fig.9a,b). However, the knockout of Abraxas clones was no longer visible by western blot analysis, although still sensitive to Olaparib. Additionally, as shown with 53BP1 knockdown, knockdown of MAD2L2 led to a decrease of Abraxas protein expression levels in cells transduced only with shMAD2L2, and in BRIP1 knockout clones, both untransduced and transduced with shMAD2L2, when compared with untransduced (Wt) mother cells (Fig.9c). Yet, it did not lead to decreased Abraxas protein expression levels in cells with BRCA1 and MAD2L2 knockdown, but it led to reduced levels in cells transduced only with shBRCA1, contrarily to the results obtained in the previous experiment (Fig.8c,9c). BRIP1 protein levels also didn't change, as upon 53BP1 knockdown (Fig.8c,9c). Consistent with the results obtain with 53BP1 knockdown, CtIP expression levels also increased, although not so clearly, in cells transduced only with shMAD2L2, co-transduced with shMAD2L2 and shBRCA1, and in Abraxas and BRIP1 knockout clones, both untransduced and transduced with shMAD2L2, when compared with untransduced (Wt) mother cells or with BRCA1-knockdown cells (Fig.8c,9c).

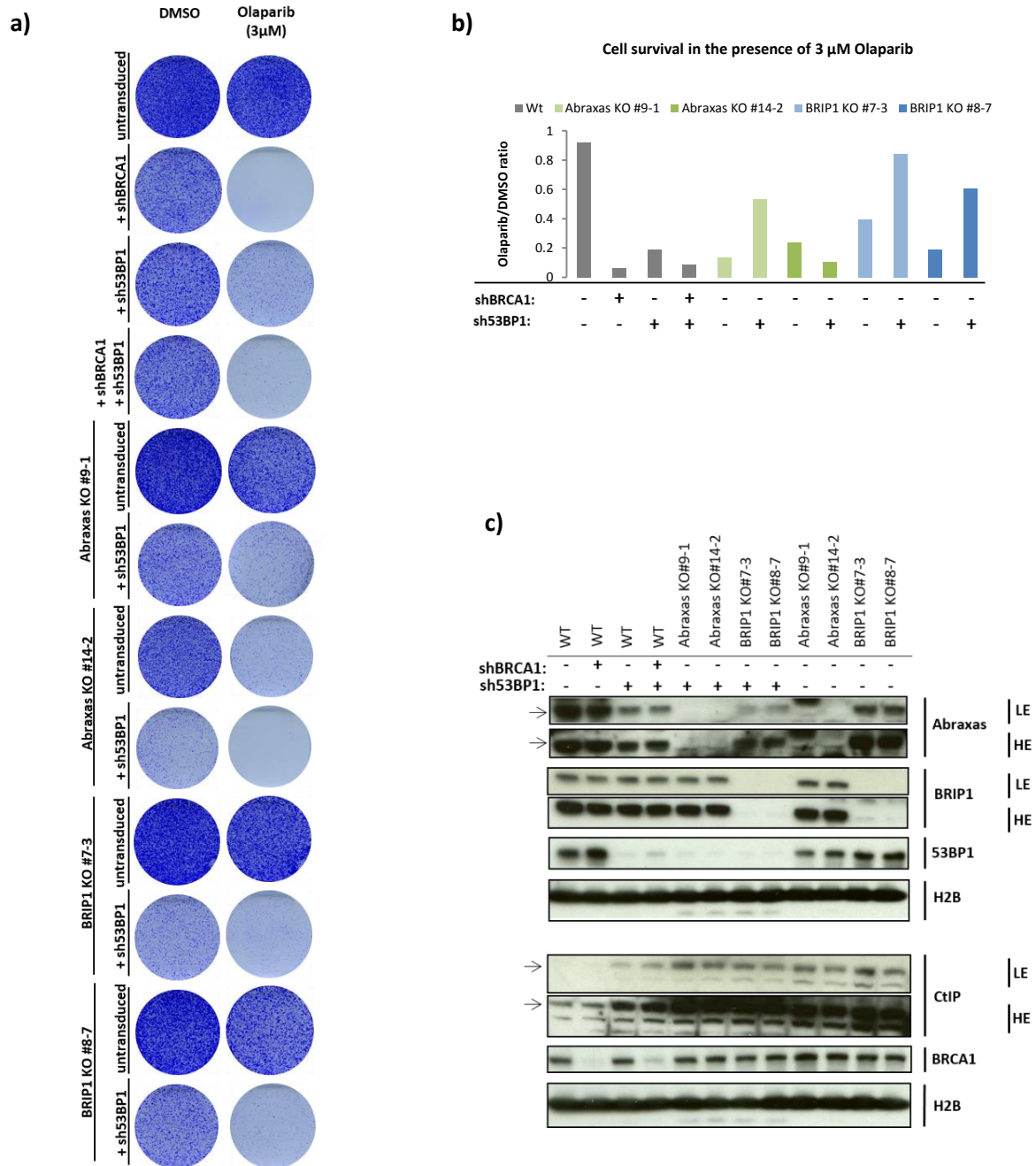


Figure 8- Knockdown of 53BP1 in knockout clones. a) Crystal violet staining of untransduced HeLa cells, HeLa cells transduced with shBRCA1 lentivirus particles, and Abraxas and BRIP1 knockout clones treated with DMSO (vehicle) or Olaparib (3µM) during 12 days, upon 53BP1 knockdown. b) Quantification of cell survival from a) by measurement of extracted crystal violet absorbance at 590 nm. Graph shows cell survival ratio between Olaparib and DMSO treatment. All values were normalized by the mean of the blank. Mean is shown from three independent measurements. c) Protein expression analysis by western blot of the cells analyzed in a). Histone H3 was blotted as a loading control. LE, low exposure; HE, high exposure.

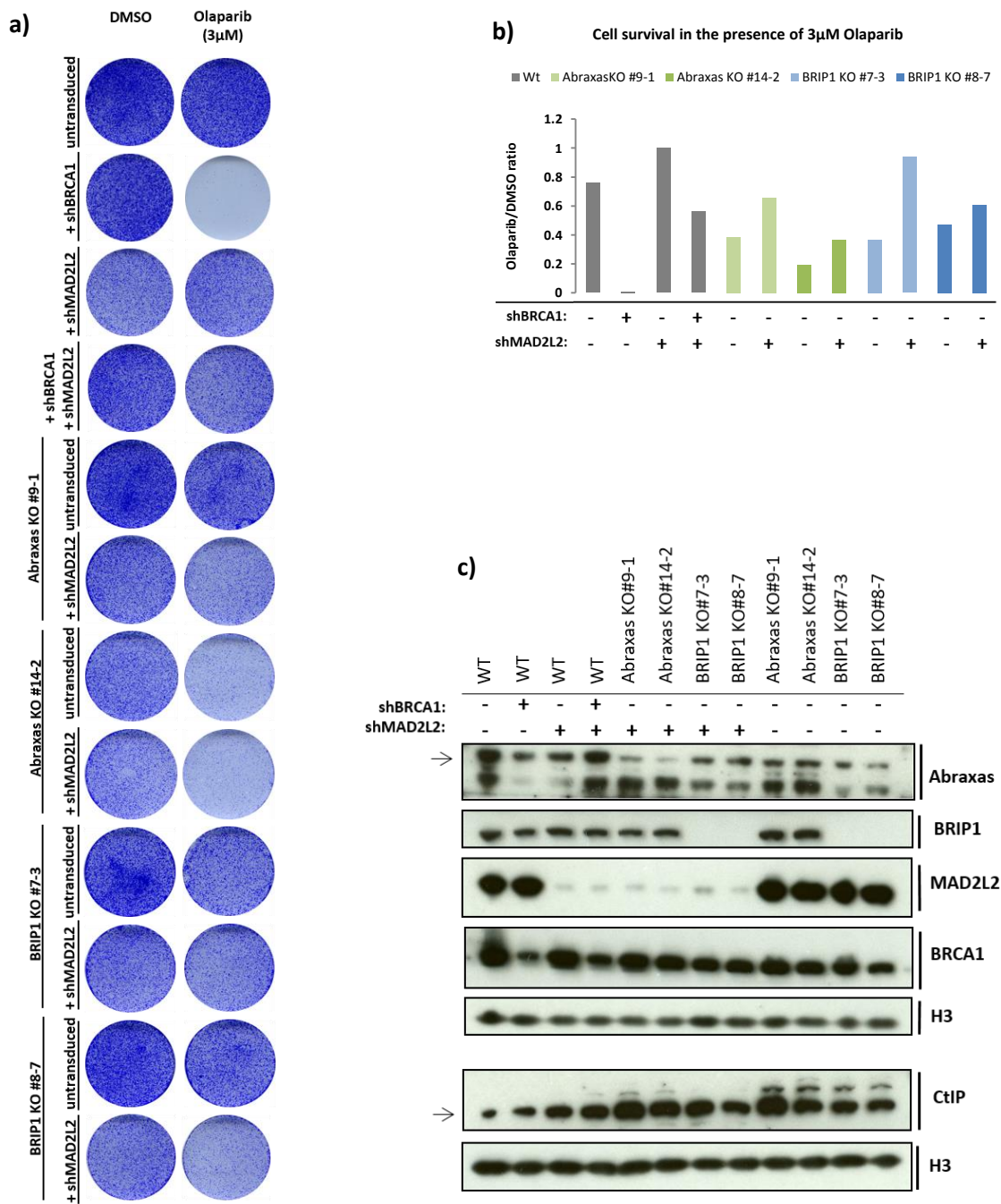


Figure 9 - Knockdown of MAD2L2 in knockout clones. a) Crystal violet staining of untransduced HeLa cells, HeLa cells transduced with shBRCA1 lentivirus particles, and Abraxas and BRIP1 knockout clones treated with DMSO (vehicle) or Olaparib (3µM) during 12 days, upon 53BP1 knockdown. b) Quantification of cell survival from a) by measurement of extracted crystal violet absorbance at 590 nm. Graph shows cell survival ratio between Olaparib and DMSO treatment. All values were normalized by the mean of the blank. Mean is shown from three independent measurements. c) Protein expression analysis by western blot of the cells analyzed in a). Histone H3 was blotted as a loading control.

4.4. Analysis of replication stress after treatment with hydroxyurea

Replication stress is the slowing or stalling of replication fork progression and/or DNA synthesis, and can be generated by a wide range of physical obstacles, usually resulting in the formation of stretches of ssDNA⁶⁵. This ssDNA frequently forms when the replicative helicase continues to unwind the parental DNA after the polymerase has stalled⁶⁶. Recently, it has been demonstrated that BRCA1 plays a role during replication stress and its loss has been shown to lead to replication fork instability³¹⁻³⁴. Thus, we decided to investigate if Abraxas and BRIP1 also play a role in replication stress response. For this end, we tested if our Abraxas and BRIP1 knockout clones would show an increase of replication stress markers after treatment with hydroxyurea (HU). HU depletes the cells of dNTPs, which initially results in stalled replication forks that, after prolonged treatment, collapse into DSBs. Therefore, we treated untransduced (Wt) mother cells, cells transduced with shBRCA1, and each two knockout clones of both Abraxas and BRIP1, for 3 hours with 2mM HU, which led to the stalling of active RFs, after which cells were fixed and pan-nuclear γ -H2AX was visualized by IF (Fig.10a). Pan-nuclear γ -H2AX reflects a generalized activation of the ATR pathway - a conserved signal transducer involved in replication stress and can be used as a marker of replication stress⁶⁷. Again, as in 4.3., the MFI of CENPF was quantified for all the cells and a threshold was set, allowing to distinguish cells in S/G2. Quantification of cells with high expression of CENPF revealed no difference between conditions in untreated cells (data not shown). Contrarily, upon treatment with 2mM HU, cells with BRCA1 knockdown and both Abraxas knockout clones showed a significant decrease of γ -H2AX relative intensity (HU/NT) when compared with untransduced (Wt) cells (Fig.10a). On the other side, only BRIP1 knockout clone #8-7 showed a reduction of γ -H2AX relative intensity, whereas #7-3 didn't show a significant difference with untransduced (Wt) cells (Fig.10a). Nevertheless, #7-3 didn't show sensitivity to Olaparib, oppositely to the other knockout clones, which might reveal that it acquired resistance and explains why this clone doesn't show a decrease of γ -H2AX like the other clones do (Fig.11a,b).

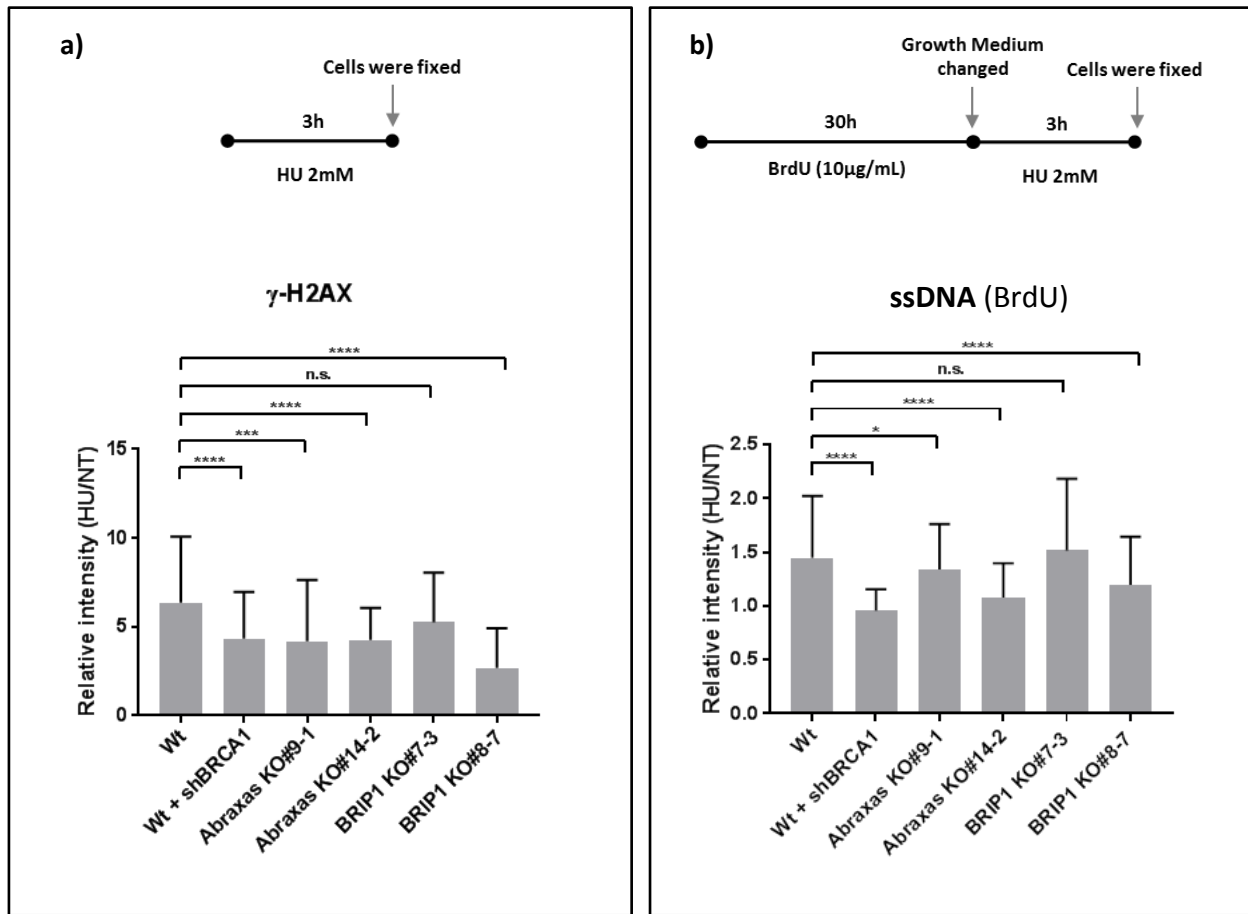


Figure 10 - Analysis of replication stress after treatment with HU. a) Quantification of MFI of γ -H2AX. Cells untreated (NT) and cells treated with 2 mM HU were fixed after 3 hours. b) Analysis of ssDNA by quantification of the MFI of BrdU. Cells were cultured with BrdU-containing medium (10 μ g/ml) for 30h, and then released in new growth medium with, or without (NT), 2mM HU and fixed after 3h. Only cells with high CENP expression were used for calculations. More than 100 cells per condition were used for calculations. The ratio between cells treated (HU) and untreated (NT) is displayed in the graphics (mean \pm s.d.). Statistical analysis was performed in GraphPad Prism 7 using a two-way ANOVA test. Results from statistical analysis of the “High CENPF” group are displayed in the graphic. n.s., not significant; *, P < 0.05; ***, P < 0.001; ****, P < 0.0001.

However, because γ -H2AX can be generated by several kinases, which detect different types of DNA damage throughout the cell cycle, pan-nuclear γ -H2AX cannot be considered a specific marker of replication stress⁶⁵. On the other hand, detection of ssDNA during S phase is a specific marker of replication stress. In order to quantify ssDNA, we cultured untransduced (Wt) mother cells, cells transduced with shBRCA1, and each two knockout clones of both Abraxas and BRIP1 in BrdU-containing medium (10 μ g/ml) for 30h, and then released in new growth medium with or without 2mM HU for 3h, after which the cells were also fixed. BrdU is a thymidine analogue that incorporates

into the DNA of cells. Visualization of ssDNA was performed with IF by using an antibody that only recognizes BrdU in ssDNA but not in dsDNA⁶⁸. Once more, MFI of CENPF was quantified for all the cells and a threshold was set, allowing to distinguish cells in S/G2. Once more, quantification of cells with high expression of CENPF revealed no difference between conditions in cells untreated (data not shown). Besides, as visualized with pan-nuclear γ -H2AX, only #7-3 didn't show significant decrease of ssDNA, when compared to untransduced (Wt) cells. Yet, this time it appeared sensitive to Olaparib, though to lesser extent than the other clones.

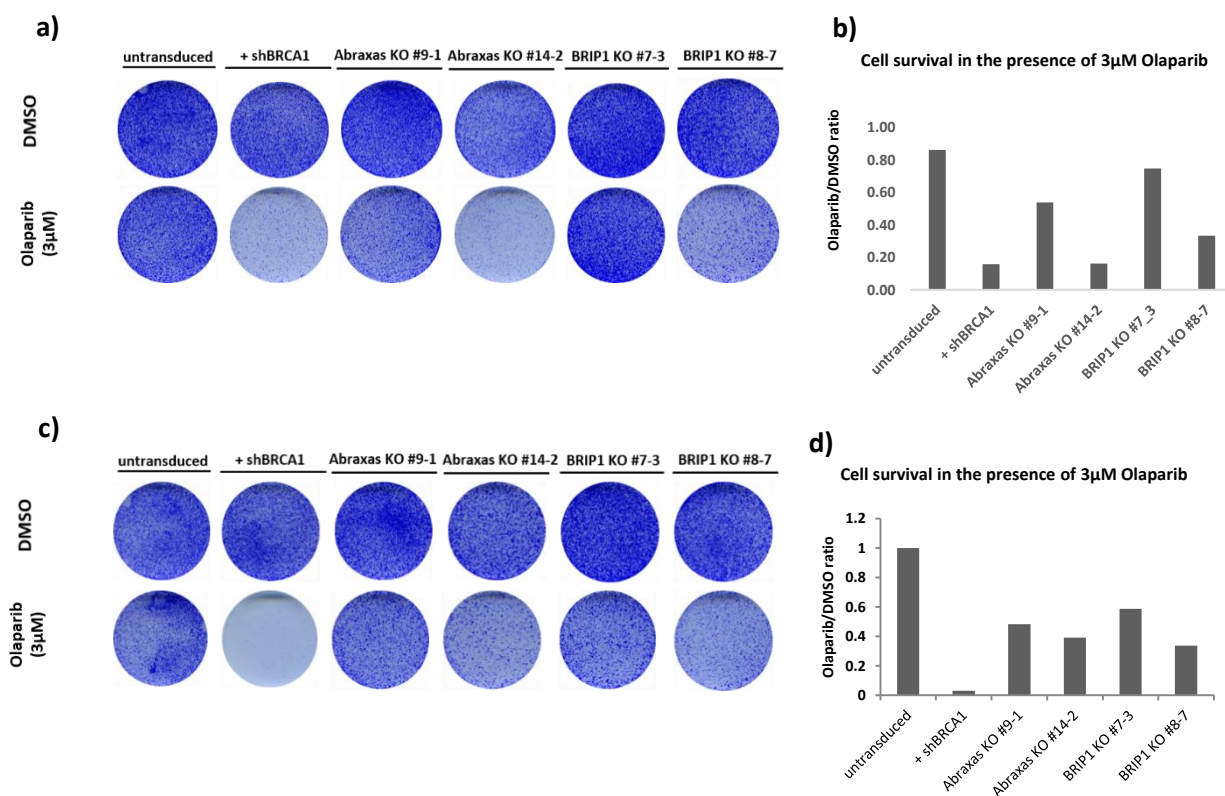


Figure 11 – Clonogenic assay in the presence of 3µM Olaparib at the time of experiments from Fig.10. a) Crystal violet staining of untransduced HeLa cells, HeLa cells transduced with shBRCA1 lentivirus particles, and Abraxas and BRIP1 knockout clones treated with DMSO (vehicle) or Olaparib (3µM) during 12 days, at the time of experiment showed in Fig.10a and c) at the time of experiment showed in Fig.10b. b), d) Quantification of cell survival from a) and c), respectively, by measurement of absorbance of crystal violet at 590 nm. Graph shows cell survival ratio between Olaparib and DMSO treatment. All values were normalized by the mean of the blank. Mean is shown from three independent measurements.

5. Discussion

Over the past 20 years, there has been considerable progress in our understanding of the biological functions of BRCA1, which has led to the development of new therapeutic approaches that target tumors with loss-of-function mutations in BRCA1. An approach that has been used to treat these tumors is to exploit the genetic concept of synthetic lethality. Inhibition of PARP1 has been shown to be synthetically lethal with deficiency of BRCA1. This observation provided the impetus for PARP1 inhibitors to be tested clinically which has recently resulted in the approval of the first PARP1 inhibitor, Olaparib, for the treatment of patients with germline mutations in *BRCA* genes. Although this approach has shown promise, multiple potential resistance mechanisms have been identified. In order to overcome this problem, a better understanding of BRCA1's molecular function and its binding partners is needed, so better therapeutic approaches can be developed. To achieve this, we decided to investigate the roles of the BRCA1-A and -B complexes in DNA repair pathway choice and in replication stress. Opposite to the BRCA1-C complex which is known to be involved in DNA end-resection, the functions of BRCA1-A and BRCA1-B is still are not well understood.

In order to study the role of BRCA1-A and -B complexes in DNA repair pathway choice and in replication stress, we used the CRISPR–Cas9 system to generate Abraxas and BRIP1 knockout clones in HeLa cells. As main adaptors of the respective binding complexes, we assume that depletion of Abraxas or BRIP1 leads to disruption of their binding complexes. The approach described here, using the incorporation of a selection marker, allowed us to have a higher efficiency. We needed to screen only a moderate number of clones in order to find the clones where the target gene was disrupted. Besides, insertion of the Blasticidin resistance cassette avoids in frame mutations, which also enhances the efficiency of this strategy.

According to our results, depletion of Abraxas or BRIP1 renders cells sensitive to PARP1 inhibition, in this case, Olaparib. These results are consistent with the idea that both BRCA1-A and –B complexes are involved in HDR. Moreover, our results show that sensitivity of Abraxas knockout clones to Olaparib is correlated with an increase of 53BP1 nuclear foci in S/G2 cell phases, upon IR-induced DNA damage, when compared with the mother cells (Wt), as it is observed in BRCA1-knockdown cells. This suggests that assembly of the BRCA1-A complex is important for inhibiting 53BP1 localization at DSBs. This is consistent with the proposed role of BRCA1-A in targeting BRCA1 to DSB sites^{44,46}. Nevertheless, only one of the Abraxas knockout clones, #14-2, showed a significant

increase of RIF1 foci formation in S/G2. We suspect that this fact is due to inter-clone heterogeneity. Indeed, clone #9-1 is less sensitive to Olaparib than #14-2, which might be explained by the lack of increase of RIF1 foci number. RIF1 accumulates at DSB sites in a manner that depends on both 53BP1 and ATM kinase activity, where ATM acts at a step between 53BP1 and RIF1, through 53BP1 phosphorylation^{10,69}. Thus, the increase of 53BP1 foci without the increase of RIF1 foci might be explain by differences in ATM expression. However, we did not confirm this experimentally. Moreover, our results also show that knockdown of 53BP1 or MAD2L2 leads to a decrease of Abraxas protein expression of BRIP1 knockout clones and in cells transduced with single sh53BP1/MAD2L2, when compared with untransduced (Wt) mother cells or untransduced BRIP1 knockout clones, respectively. Because, when 53BP1 or MAD2L2 are silenced, NHEJ can't proceed, BRCA1 does not need to displace 53BP1 from DNA DSBs site. This might explain why Abraxas is underexpressed when these proteins are silenced, as it is no longer required for BRCA1 localization at DSBs. Further experiments are required in order to understand how Abraxas expression or stability is control in these conditions. Inconsistently, cells in which BRCA1 was silenced did not behave equally in both experiments, showing decreased Abraxas protein expression only in the second experiment (shMAD2L2), whereas Abraxas protein expression levels remained the same as in Wt mother cells in the first experiment (sh53BP1). Moreover, co-knockdown of BRCA1 and 53BP1, but not BRCA1 and MAD2L2, led to underexpression of Abraxas, when compared with untransduced (Wt) mother cells. This is probably due to differences in the roles played in DDR, between 53BP1 and MAD2L2. It should also be noticed that CtIP protein expression levels are slightly overexpressed in Abraxas knockout clone #9-1, which can also explain why this clone is less sensitive, in comparison with #14-2. Although our results show that knockdown of 53BP1 leads to lethality in Olaparib, and does not rescue either BRCA1-knockdown cells or #14-2, the Abraxas knockout clone #9-1 was slightly rescued by 53BP1 knockdown. Nevertheless, these results are inconclusive and the lethality upon transduction with sh53BP1, observed in the presence of Olaparib, might be a result of an off-target effect. Oppositely, silencing MAD2L2 did rescue BRCA1 knockdown cells and both Abraxas knockout clones. These results are consistent with the hypothesis that the BRCA1-A complex functions upstream of end resection. However, protein expression analysis of the cells used in these experiment (shMAD2L2), reveals that Abraxas knockout clones express Abraxas, though in low levels. This might be due to expression of an isoform, as an adaptation mechanism. Alternatively, because HeLa cells are known to have complex chromosomal aberrations and to be aneuploid, we speculate HeLa cells might have more than only two copies of *ABRAXAS* gene, and that the depletion of the gene by CRISPR-Cas9 was

not effective in all gene copies, which led to residual expression of the gene. In order to confirm Abraxas's role in pathway choice, further experiments are required, such as analysis of BRCA1, RAD51 and Abraxas foci formation after IR exposure, when 53BP1 or MAD2L2 are silenced, and analysis of 5' end resection to monitor HRR in Abraxas knockout clones. On the other hand, BRIP1 knockout clones displayed opposite results to Abraxas knockout clones when 53BP1 and RIF1 foci formation was quantified. Only BRIP1 knockout #8-7 showed significant increase of 53BP1 foci formation in S/G2, when compared with untransduced (Wt) mother cells. Indeed, clone #7-3 is the less sensitive clone to Olaparib. These results are consistent with the previous statement that 53BP1 foci formation in S/G2 after IR, is correlated with sensitivity to PARP1 inhibition. In spite of this, both BRIP1 knockout clones revealed a significant increase in RIF1 foci formation, upon IR-induced DNA damage. Because, as referred before, RIF1 accumulation at DSBs is dependent on 53BP1, it is difficult to formulate an explanation of how RIF1 forms foci without its upstream partner, 53BP1, localizing at DSBs. Different functions between 53BP1 and RIF1 in pathway choice might explain this observations. As suggested above, these differences between BRIP1 knockout clones can be a result of inter-clone heterogeneity. Furthermore, BRIP1 untransduced knockout cells display decreased Abraxas protein expression, when compared to Wt mother cells. The same was not observed in Abraxas knockout clones, where BRIP1 expression remained the same as in the Wt mother cells. These results suggest that BRIP1 expression, or the assembly of the respective complex, might control, directly or indirectly, the stability of Abraxas. Further investigation of this mechanism is required to confirm our results. Silencing of both 53BP1 or MAD2L2 led to the rescue of the lethality under Olaparib of both BRIP1 knockout clones, indicating that BRIP1 is also involved in the pathway choice, in steps upstream of end resection. Nevertheless, similar to what was mentioned above, analysis of BRCA1, RAD51 and BRIP1 foci formation after IR exposure, when 53BP1 or MAD2L2 are silenced, and analysis of 5' end resection to monitor HRR in BRIP1 knockout clones should be performed in order to confirm these results. Taking together our results, further experiments should be carried out with the aim of understanding if the role in pathway choice of BRCA1-A and -B is cell cycle specific, as BRIP1 has been reported to be involved in replication checkpoint control, whereas Abraxas is involved in G2/M checkpoint control.

Replication stalling is at the heart of many chemotherapeutic agents, including the ones that block replication fork progression, as PARP inhibitors. BRCA1 has recently been shown to be involved in replication stress, where it is involved in stabilization of RAD51 at stalled replication forks to protect nascent strands from MRE11-dependent degradation³²⁻³⁴. Consequently, it was shown that

RF protection in BRCA1-deficient cells can lead to resistance to PARP inhibition³¹. Hence, we decided to investigate if the BRCA1-forming complexes A and B also play a role in the replication stress response. Our results show a consistent display of pan-nuclear γ -H2AX upon treatment with fork stalling agents, i.e. HU. However, cells transduced with shBRCA1, both Abraxas KO clones and one of BRIP1 knockout clones (#8-7) showed a decrease in intensity, compared with untransduced (Wt) mother cells. A reduction in pan-nuclear γ -H2AX in cells deficient in BRCA1 or BRIP1 is consistent with the idea that BRCA1-B is involved in replication stress response, as its assembly is necessary for ATR-dependent phosphorylation events, such as the phosphorylation of H2AX. On the other hand, the reduction of intensity observed in Abraxas knockout clones might reveal a novel role of BRCA1-A in replication stress response. The same pattern was observed when ssDNA was quantified, where cells transduced with shBRCA1, both Abraxas KO clones and one of BRIP1 knockout clones (#8-7) showed a decrease in ssDNA, compared with untransduced (Wt) mother cells. The results observed in cells where BRCA1 is silenced can be explained by the instability caused by the lack of fork protection when BRCA1 is absent. Thus, MRE11 is able to access the stalled fork, leading to RF degradation, which might explain the decrease of ssDNA. Consequently, the decrease in Abraxas and BRIP1 knockout might indicate that these complexes are involved in BRCA1's function in protecting the fork. Hence, further experiments should be carried out in order to confirm these results, such as co-localization of ssDNA with MRE11 and measurement of DNA synthesis using DNA fiber or DNA combing assays.

6. Conclusion and Future Perspectives

Together, our results show that depletion of either Abraxas or BRIP1, and thus, disruption of the respective complexes, is synthetically lethal with PARP1 inhibition. We suggest that this phenotype is a result of the role played by BRCA1-A and BRCA1-B in HDR, more specifically, in the DNA repair pathway choice. Moreover, BRIP1 expression, or the assembly of BRCA1-B, appears to influence the expression of Abraxas. Here, we also propose a role in replication stress response played by BRCA1-A and –B complexes. However, further investigation is needed to validate our findings.

The gain of insight into BRCA1 complexes is mostly based on experiments that study each complex separately. Here we perform a “side-by-side” analysis of both complexes, allowing a more trustable analysis by eliminating the variability between studies. Nevertheless, all the experiments here shown were performed using the same tumor-derived cell line, HeLa. Thus, it is also necessary to verify if these results are reproducible in other cell lines. Additionally, the observed high variability between the knockout clones for the same gene, which could be potentially explained by off-targets effects. A higher number of sgRNAs per gene could be used to overcome this problem. We also suggest to use a cell line with a well-defined karyotype, where the number of gene copies is known, in order to be sure the knockout of the gene is present in homozygosity. To assure this, we suggest the use of haploid cells, such as HAP1 cell line.

In order to better understand the functions of these complexes, a systematic analysis of all the components that form each complex is necessary. Furthermore, it is also important to understand what is the role of the binding of BRCA1 in these complexes, and if it is essential for the functions played by the complexes. Likewise, it still remains unknown if the complexes can regulate each other. Finally, it still remains unknown how BRCA1-A and –B act in response to PARP1 inhibition. Thus, a full understanding of BRCA1 and its binding partners’ role in DNA repair and replication stress can help to understand new ways of resistance to the current drugs used in BRCA-deficient cells, and to improve the current therapeutic approaches.

7. References

1. Jackson, S. P. & Bartek, J. The DNA-damage response in human biology and disease. *Nature* **461**, 1071–8 (2009).
2. Rouse, J. & Jackson, S. P. Interfaces Between the Detection, Signaling, and Repair of DNA Damage. *Science (80-.)*. **297**, 547–551 (2002).
3. Harrison, J. C. & Haber, J. E. Surviving the Breakup: The DNA Damage Checkpoint. *Annu. Rev. Genet.* **40**, 209–235 (2006).
4. Fagagna, F. d'Adda di *et al.* A DNA damage checkpoint response in telomere-initiated senescence. *Nature* **426**, 194–198 (2003).
5. Kang, C. *et al.* The DNA damage response induces inflammation and senescence by inhibiting autophagy of GATA4. *Science (80-.)*. **349**, aaa5612-aaa5612 (2015).
6. Khanna, K. K. & Jackson, S. P. DNA double-strand breaks: signaling, repair and the cancer connection. *Nat. Genet.* **27**, 247–54 (2001).
7. Chapman, J. R., Taylor, M. R. G. & Boulton, S. J. Playing the End Game: DNA Double-Strand Break Repair Pathway Choice. *Mol. Cell* **47**, 497–510 (2012).
8. Symington, L. S. & Gautier, J. Double-Strand Break End Resection and Repair Pathway Choice. *Annu. Rev. Genet.* **45**, 247–271 (2011).
9. Zimmermann, M., Lottersberger, F., Buonomo, S. B., Sfeir, A. & de Lange, T. 53BP1 Regulates DSB Repair Using Rif1 to Control 5' End Resection. *Science (80-.)*. **339**, 700–704 (2013).
10. Escribano-Díaz, C. *et al.* A Cell Cycle-Dependent Regulatory Circuit Composed of 53BP1-RIF1 and BRCA1-CtIP Controls DNA Repair Pathway Choice. *Mol. Cell* **49**, 872–883 (2013).
11. Chapman, J. R. *et al.* RIF1 Is Essential for 53BP1-Dependent Nonhomologous End Joining and Suppression of DNA Double-Strand Break Resection. *Mol. Cell* **49**, 858–871 (2013).
12. Callen, E. *et al.* 53BP1 Mediates Productive and Mutagenic DNA Repair through Distinct Phosphoprotein Interactions. *Cell* **153**, 1266–1280 (2013).
13. Boersma, V. *et al.* MAD2L2 controls DNA repair at telomeres and DNA breaks by inhibiting 5' end resection. *Nature* **521**, 537–40 (2015).
14. Xu, G. *et al.* REV7 counteracts DNA double-strand break resection and affects PARP inhibition. *Nature* **521**, 541–544 (2015).
15. Lieber, M. R. The mechanism of double-strand DNA break repair by the nonhomologous DNA end-joining pathway. *Annu Rev Biochem* 181–211 (2010). doi:10.1146/annurev.biochem.052308.093131.The
16. Nakamura, K. *et al.* Collaborative action of Brca1 and CtIP in elimination of covalent modifications from double-strand breaks to facilitate subsequent break repair. *PLoS Genet.* **6**, (2010).

17. Heyer, W.-D., Ehmsen, K. T. & Liu, J. Regulation of Homologous Recombination in Eukaryotes. *Annu. Rev. Genet.* **44**, 113–139 (2010).
18. Feng, L., Fong, K. W., Wang, J., Wang, W. & Chen, J. RIF1 counteracts BRCA1-mediated end resection during DNA repair. *J. Biol. Chem.* **288**, 11135–11143 (2013).
19. Moynahan, M. E. & Jasin, M. Mitotic homologous recombination maintains genomic stability and suppresses tumorigenesis. *Nat. Rev. Mol. Cell Biol.* **11**, 196–207 (2010).
20. Panier, S. & Durocher, D. Push back to respond better: regulatory inhibition of the DNA double-strand break response. *Nat. Rev. Mol. Cell Biol.* **14**, 661–672 (2013).
21. Lord, C. J. & Ashworth, A. Mechanisms of resistance to therapies targeting BRCA-mutant cancers. *Nat. Med.* **19**, 1381–8 (2013).
22. Kaelin, W. G. The Concept of Synthetic Lethality in the Context of Anticancer Therapy. *Nat. Rev. Cancer* **5**, 689–698 (2005).
23. Farmer, H. *et al.* Targeting the DNA repair defect in BRCA mutant cells as a therapeutic strategy. *Nature* **434**, 917–21 (2005).
24. ter Brugge, P. *et al.* Mechanisms of Therapy Resistance in Patient-Derived Xenograft Models of BRCA1-Deficient Breast Cancer. *J. Natl. Cancer Inst.* **108**, djw148 (2016).
25. Nnunziato, S. T. A., Arazas, M. A. B., Ottenberg, S. V. E. N. R. & Onkers, J. O. S. J. Genetic Dissection of Cancer Development , Therapy Response , and Resistance in Mouse Models of Breast Cancer. **LXXXI**, (2016).
26. Patch, A.-M. *et al.* Whole-genome characterization of chemoresistant ovarian cancer. *Nature* **521**, 489–494 (2015).
27. Bouwman, P. *et al.* 53BP1 loss rescues BRCA1 deficiency and is associated with triple-negative and BRCA-mutated breast cancers. *Nat. Struct. Mol. Biol.* **17**, 688–695 (2010).
28. Bunting, S. F. *et al.* 53BP1 inhibits homologous recombination in *brca1*-deficient cells by blocking resection of DNA breaks. *Cell* **141**, 243–254 (2010).
29. Wang, J. *et al.* PTIP associates with artemis to dictate DNA repair pathway choice. *Genes Dev.* **28**, 2693–2698 (2014).
30. Drané, P., Brault, M., Cui, G. & Meghani, K. TIRR regulates 53BP1 by masking its histone methyl-lysine binding function. *Nat. Publ. Gr.* 1–37 (2017). doi:10.1038/nature21358
31. Ray Chaudhuri, A. *et al.* Replication fork stability confers chemoresistance in BRCA-deficient cells. *Nature* **535**, 382–387 (2016).
32. Schlacher, K., Wu, H. & Jasin, M. A Distinct Replication Fork Protection Pathway Connects Fanconi Anemia Tumor Suppressors to RAD51-BRCA1/2. *Cancer Cell* **22**, 106–116 (2012).
33. Pathania, S. *et al.* BRCA1 haploinsufficiency for replication stress suppression in primary cells. *Nat. Commun.* **5**, 5496 (2014).

34. Pathania, S. *et al.* BRCA1 is required for postreplication repair after UV-induced DNA damage. *Mol. Cell* **44**, 235–251 (2011).
35. Huen, M. S. Y., Sy, S. M. H. & Chen, J. BRCA1 and its toolbox for the maintenance of genome integrity. *Nat. Rev. Mol. Cell Biol.* **11**, 138–148 (2010).
36. Wang, B. BRCA1 tumor suppressor network: focusing on its tail. *Cell Biosci.* **2**, 6 (2012).
37. Her, J., Soo Lee, N., Kim, Y. & Kim, H. Factors forming the BRCA1-A complex orchestrate BRCA1 recruitment to the sites of DNA damage. *Acta Biochim. Biophys. Sin. (Shanghai)*. **48**, 658–664 (2016).
38. Joukov, V., Chen, J., Fox, E. A., Green, J. B. A. & Livingston, D. M. Functional communication between endogenous BRCA1 and its partner, BARD1, during *Xenopus laevis* development. *Proc. Natl. Acad. Sci.* **98**, 12078–12083 (2001).
39. Fabbro, M., Rodriguez, J. A., Baer, R. & Henderson, B. R. BARD1 induces BRCA1 intranuclear foci formation by increasing RING-dependent BRCA1 nuclear import and inhibiting BRCA1 nuclear export. *J. Biol. Chem.* **277**, 21315–21324 (2002).
40. Morris, J. R. & Solomon, E. BRCA1: BARD1 induces the formation of conjugated ubiquitin structures, dependent on K6 of ubiquitin, in cells during DNA replication and repair. *Hum. Mol. Genet.* **13**, 807–817 (2004).
41. Sartori, A. A. *et al.* Human CtIP promotes DNA end resection. *Nature* **450**, 509–514 (2007).
42. Cruz-García, A., López-Saavedra, A. & Huertas, P. BRCA1 accelerates CtIP-mediated DNA-end resection. *Cell Rep.* **9**, 451–459 (2014).
43. Wang, J. *et al.* Loss of CtIP disturbs homologous recombination repair and sensitizes breast cancer cells to PARP inhibitors. *Oncotarget* **5**, 7701–7714 (2015).
44. Wang, B. *et al.* Abraxas and RAP80 Form a BRCA1 Protein Complex Required for the DNA Damage Response. **316**, 1194–1198 (2007).
45. Castillo, A. *et al.* The BRCA1-interacting protein Abraxas is required for genomic stability and tumor suppression. *Cell Rep.* **8**, 807–817 (2014).
46. Liu, Z., Wu, J. & Yu, X. CCDC98 targets BRCA1 to DNA damage sites. **14**, 716–720 (2007).
47. Coleman, K. A. & Greenberg, R. A. The BRCA1-RAP80 complex regulates DNA repair mechanism utilization by restricting end resection. *J. Biol. Chem.* **286**, 13669–13680 (2011).
48. Ng, H. M., Wei, L., Lan, L. & Huen, M. S. Y. The Lys63-deubiquitylating enzyme BRCC36 limits DNA break processing and repair. *J. Biol. Chem.* **291**, 16197–16207 (2016).
49. Hu, Y. *et al.* PARP1-driven poly-ADP-ribosylation regulates BRCA1 function in homologous recombination-mediated DNA repair. *Cancer Discov.* **4**, 1430–47 (2014).
50. Kim, H., Huang, J. & Chen, J. CCDC98 is a BRCA1-BRCT domain – binding protein involved in the DNA damage response. **14**, (2007).

51. Greenberg, R. A. *et al.* Multifactorial contributions to an acute DNA damage response by BRCA1 / BARD1-containing complexes. 34–46 (2006). doi:10.1101/gad.1381306.)
52. Gong, Z., Kim, J. E., Leung, C. C. Y., Glover, J. N. M. & Chen, J. BACH1/FANCI Acts with TopBP1 and Participates Early in DNA Replication Checkpoint Control. *Mol. Cell* **37**, 438–446 (2010).
53. Yu, X., Christiano, C., Chini, S. & He, M. The BRCT Domain Is a Phospho-Protein Binding Domain. **302**, (2003).
54. Cantor, S. B. *et al.* BACH1 , a Novel Helicase-like Protein , Interacts Directly with BRCA1 and Contributes to Its DNA Repair Function. **105**, 149–160 (2001).
55. Peng, M. *et al.* The FANCI / MutL a interaction is required for correction of the cross-link response in FA-J cells. **26**, 3238–3249 (2007).
56. Xie, J. *et al.* Targeting the FANCI-BRCA1 interaction promotes a switch from recombination to poleta-dependent bypass. *Oncogene* **29**, 2499–508 (2010).
57. Apostolou, P. & Fostira, F. Hereditary breast cancer: the era of new susceptibility genes. *Biomed Res. Int.* **2013**, 747318 (2013).
58. Pennington, K. P. *et al.* Germline and Somatic Mutations in Homologous Recombination Genes Predict Platinum Response and Survival in Ovarian, Fallopian Tube, and Peritoneal Carcinomas. *Clin. Cancer Res.* **20**, (2014).
59. Maxwell, K. N. & Nathanson, K. L. Common breast cancer risk variants in the post-COGS era: a comprehensive review. *Breast Cancer Res.* **15**, 212 (2013).
60. Cantor, S. B. & Guillemette, S. Hereditary breast cancer and the BRCA1-associated FANCI/BACH1/BRIP1. *Future Oncol.* **7**, 253–61 (2011).
61. Sakuma, T., Nishikawa, A., Kume, S., Chayama, K. & Yamamoto, T. Multiplex genome engineering in human cells using all-in-one CRISPR/Cas9 vector system. *Sci. Rep.* **4**, 5400 (2015).
62. Cong, L. *et al.* Multiplex Genome Engineering Using CRISPR/Cas Systems. *Science (80-.).* **339**, 819–823 (2013).
63. Lackner, D. H. *et al.* A generic strategy for CRISPR-Cas9-mediated gene tagging. *Nat. Commun.* **6**, 10237 (2015).
64. Liao, H., Winkfein, R. J., Mack, G., Rattner, J. B. & Yen, T. J. CENP-F is a protein of the nuclear matrix that assembles onto kinetochores at late G2 and is rapidly degraded after mitosis. *J. Cell Biol.* **130**, 507–18 (1995).
65. Zeman, M. K. & Cimprich, K. A. Causes and consequences of replication stress. *Nat. Cell Biol.* **16**, 2–9 (2014).
66. Pacek, M. & Walter, J. C. A requirement for MCM7 and Cdc45 in chromosome unwinding during eukaryotic DNA replication. *EMBO J.* **23**, 3667–3676 (2004).
67. Toledo, L. I. *et al.* A cell-based screen identifies ATR inhibitors with synthetic lethal properties

for cancer-associated mutations. *Nat. Struct. Mol. Biol.* **18**, 721–727 (2011).

68. Raderschall, E., Golub, E. I. & Haaf, T. Nuclear foci of mammalian recombination proteins are located at single-stranded DNA regions formed after DNA damage. *Proc. Natl. Acad. Sci. U. S. A.* **96**, 1921–6 (1999).
69. Silverman, J., Takai, H., Buonomo, S. B. C., Eisenhaber, F. & de Lange, T. Human Rif1, ortholog of a yeast telomeric protein, is regulated by ATM and 53BP1 and functions in the S-phase checkpoint. *Genes Dev.* **18**, 2108–2119 (2004).